JOC The Journal of Organic Chemistry

pubs.acs.org/joc Article

Syntheses and Aromaticity Parameters of Hexahydroxypyrrocorphin, Porphotrilactones, and Their Oxidation State Intermediates

Nisansala Hewage, Matthew J. Guberman-Pfeffer, Nivedita Chaudhri, Matthias Zeller, José A. Gascón, and Christian Brückner*

Cite This: J. Org. Chem. 2022, 87, 12096−12108 Read Online

ACCESS | Metrics & More | Article Recommendations | Supporting Information

ABSTRACT: Triple OsO_4-mediated dihydroxylation of *meso*-tetrakis(pentafluorophenyl)porphyrin formed a non-aromatic hexahydroxypyrrocorphin as a single stereo-isomer. A one-step oxidative conversion of all three diol functionalities to lactone moieties generated three out of the four possible porphotrilactone regioisomers that were spectroscopically and structurally characterized. This conversion recovered most of the porphyrinic macrocycle aromatic ring current, as seen in their ^{1}H NMR spectra and modeled using DFT computations. Stepwise OsO_4-mediated dihydroxylations of porpho-mono- and -di-lactones generated intermediate oxidation state compounds between the pyrrole-three pyrroline macrocycle of the pyrrocorphin and the pyrrole-three oxazolone chromophore of the trilactones. The aromaticity of these chromophores was reduced with increasing number of oxazolone to pyrroline replacements, showing the importance for the presence of three lactone moieties for the retention of the macrocycle aromaticity in the tris-β,β'-modified macrocycles. This work first describes hexahydoxypyrrocorphins, porphotrislactones, and the oxidation state intermediates between them; furthers the understanding of the roles of β-lactone moieties in the expression of porphyrinic macrocycle aromaticity; and generally broadens access to chemically stable pyrrocorphins and pyrrocorphin analogues.

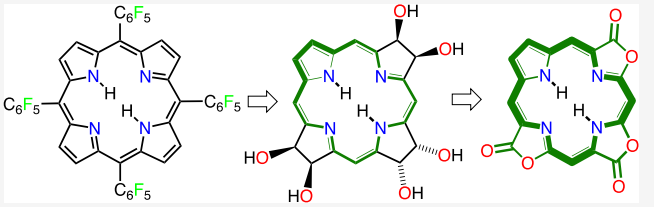

INTRODUCTION

Sequential conversion of up to 2 cross-conjugated β,β'-double bonds of the 18 + 4 π-aromatic system of a porphyrin to single bonds through reduction, oxidation, or addition reactions generates chlorins, bacteriochlorins, or isobacteriochlorins (Figure 1).[1] In all cases, the inner 18 π-electron Hückel-aromatic system responsible for the characteristic electronic properties of the hydroporphyrins is retained.[2]

One such conversion reaction is the OsO_4-mediated dihydroxylation of *meso*-arylporphyrins (or their metal complexes). Controlled by the stoichiometric ratio of porphyrin to OsO_4, this reaction generates β,β'-dihydroxylated chlorins[3] and regioselectively[4] tetrahydroxylated bacteriochlorins[5] or metalloisobacteriochlorins (both as mixtures of stereoisomers).[6] All these chromophores conform to the electronic properties expected for their hydroporphyrin class. Applied to free-base *meso*-tetrakis(pentafluorophenyl)-porphyrin $\mathbf{1}^{\mathbf{F}}$, chlorin $\mathbf{2}^{\mathbf{F}}$ and bacteriochlorin stereoisomers $\mathbf{3}^{\mathbf{F}}$ are generated (Scheme 1).[3,5,6] The β,β'-dihydroxylated pyrroline moieties also proved to be versatile synthetic handles for a range of transformations, generating, inter alia, porphyrinoids containing non-pyrrolic heterocycles.[7]

One reaction that converts the β,β'-dihydroxypyrroline-based hydroporphyrins to pyrrole-modified porphyrins is their oxidation. Thus, chlorin diol $\mathbf{2}^{\mathbf{F}}$ or bacteriochlorin tetraol $\mathbf{3}^{\mathbf{F}}$ can be converted to porpholactone $\mathbf{4}^{\mathbf{F}}$ and bacteriodilactone regioisomers $\mathbf{5}^{\mathbf{F}}$, respectively (Scheme 1).[6,8] Equivalent syntheses of isobacteriodilactone isomers are available as well.[6] A number of alternate syntheses of these oxazolone-containing porphyrin analogues have also been reported.[9] Free-base and metalated porpholactones found broad utility in catalysis,[10] as chlorophyll or heme models,[11] as lanthanide sensitizers,[12] in bioimaging,[12] in photochemotherapeutics,[13] as phototheranostic agents,[14] as oxygen-sensing dyes,[15] or as optical chemosensors.[16] The electronic influence of the lactone moieties on the chromophore was studied in some detail.[8,9b,11a,17]

Importantly, removal of a third β,β'-double bond from a porphyrin generates the non-aromatic hexahydroporphyrins (Figure 2). These can exist as two tautomers: the non-macrocycle-conjugated leuco form, the porphyrinogen (often preferred for the free bases), or as a macrocycle-conjugated but

Received: May 22, 2022
Published: September 6, 2022

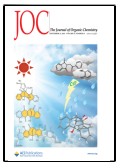

https://doi.org/10.1021/acs.joc.2c01202
J. Org. Chem. 2022, 87, 12096−12108

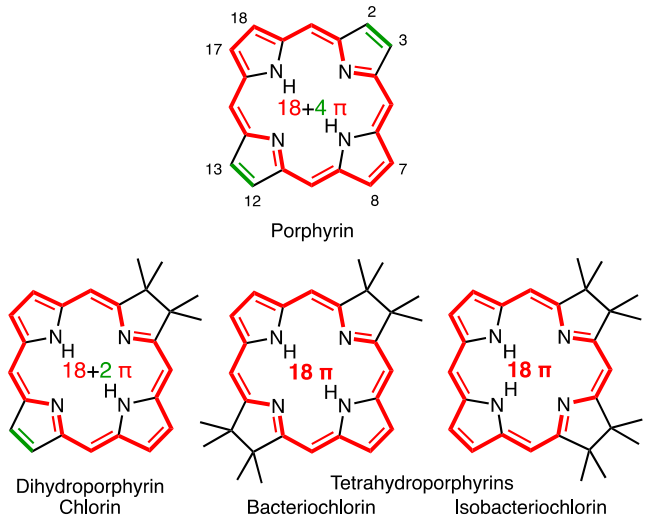

Figure 1. Framework structures of the hydroporphyrin classes indicated and the numbering system used. Aromatic macrocycle π-systems are highlighted in red, and cross-conjugated double bonds are highlighted in green.

Scheme 1. Stepwise Formation of *meso*-Tetrakis(pentafluorophenyl)-mono- and Bis-porpholactones via a Two-Step Oxidation of the Corresponding *meso*-Tetrakis(pentafluorophenyl)porphyrin

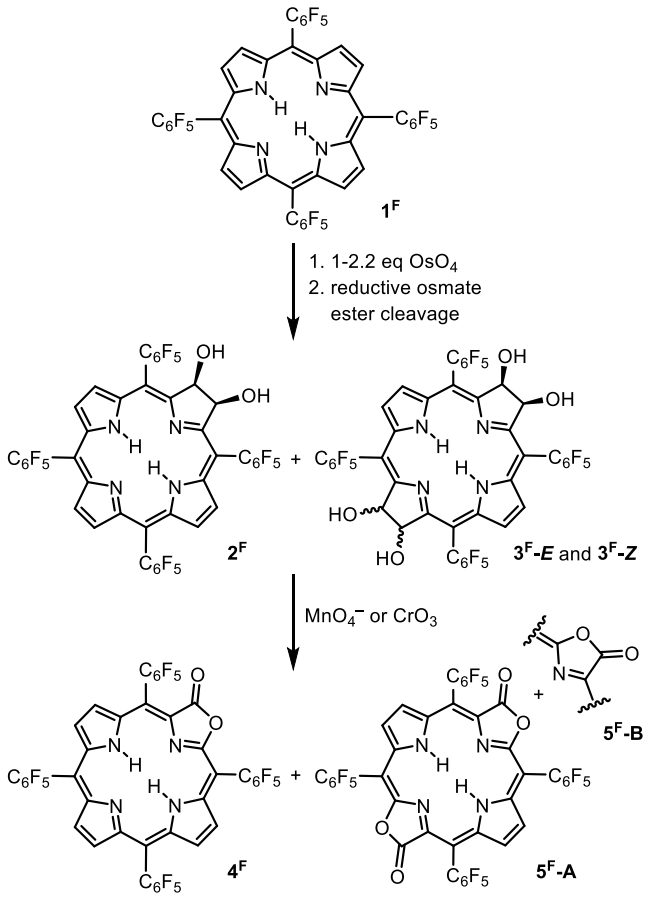

non-aromatic pyrrocorphin (often preferred for the nickel complexes).[18] The pyrrocorphins were discovered to be precursors in the biosynthesis of vitamin B_{12}.[18c,19] They were thus subject of numerous studies by the group of

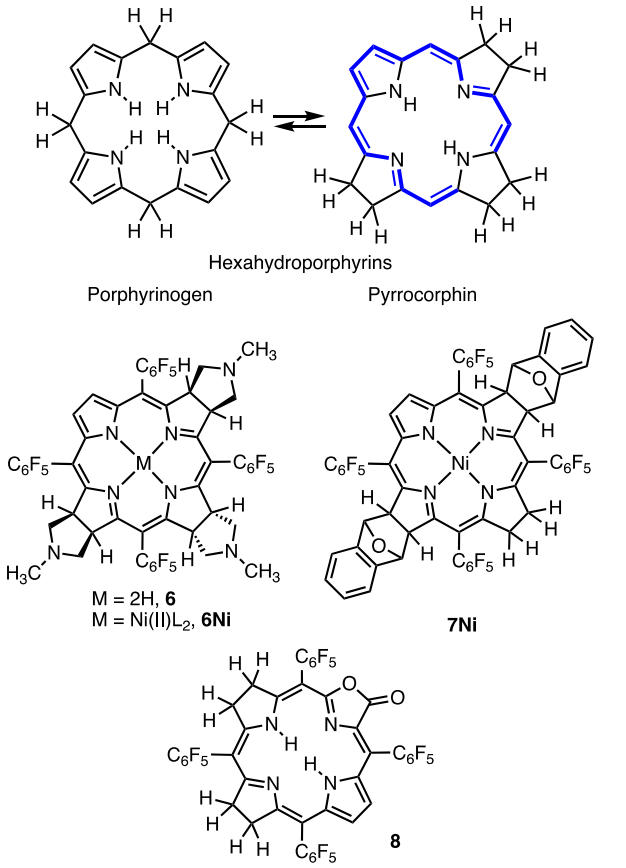

Figure 2. Structure and tautomeric equilibrium found in the pyrrocorphins. The conjugated but non-aromatic π-system of the pyrrocorphin is highlighted in blue. Representative literature-known (metallo)pyrrocorphins **6**/**6Ni**,[24] **7Ni**,[25] and analogue **8**.[26]

Eschenmoser[18b,c,20] and Batters-by.[19] These included detailed structural investigations of the nickel complexes of (hexa)-hydroporphyrins.[21] The diatropic ring currents of the nickel pyrrocorphins, as measured by ^{1}H NMR spectroscopic shifts, were recorded by the group of Smith.[22] The group of Stolzenberg reported a series of studies on the formation and redox chemistry of (multiple isomers of) octaethyl-tetra- and -hexa-hydroporphyrin metal complexes.[18e,23] The exquisite sensitivity of the pyrrocorphins (as well as porphyrinogens) toward oxidation distinguishes these systems from the much more robust chlorins, bacteriochlorins, and isobacteriochlorins.

The conversion of porphyrins to pyrrocorphins includes the formation of 1,3-dipolar cycloaddition tris-adducts, such as **6**/**6Ni**,[24] or the reduction of a bacteriochlorin bis-adduct **7Ni**.[25] Porpholactones with more than two lactone moieties have not been reported to date, although mixed tris-modified systems, such as compound **8**, have become known.[26] Other tris-substituted systems are the octaethyltriketones prepared by the oxidation of octaethylporphyrin.[27]

Using *meso*-tetrakis(pentafluorophenyl)porphyrin $\mathbf{1}^{\mathbf{F}}$, we expand here the OsO_4-mediated dihydroxylation of porphyrins to the generation of a non-macrocycle-aromatic tris-dihydroxylated pyrrocorphin. Further, the oxidation of the hexahydroxypyrrocorphin generated three isomers of the novel trilactones, thus expanding the porpholactone landscape. These novel trilactones are aromatic with stark differences between the isomers, providing a second example of how β-oxo-substituents change the π-electron conjugation pathway to generate an

https://doi.org/10.1021/acs.joc.2c01202
J. Org. Chem. 2022, 87, 12096−12108

Scheme 2. Synthesis of Hexahydroxypyrrocorphin 9 and Its Oxidative Conversion to a Mixture of the Three Isomeric Porphotrilactone Isomers 10[a]

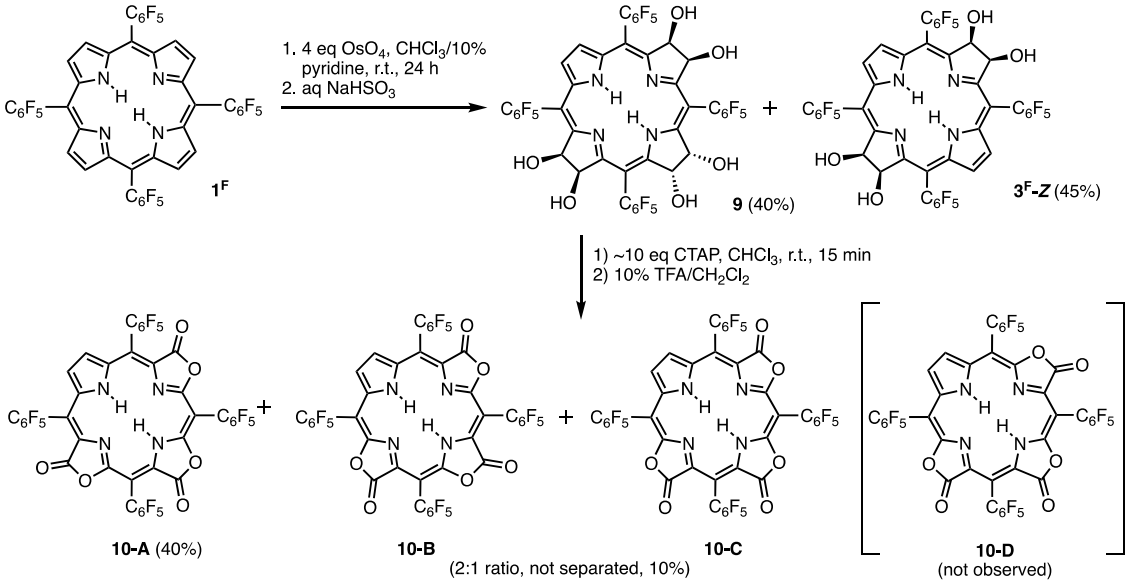

[a]CTAP = cetyl$(Me)_3N^+MnO_4^-$.

aromatic macrocycle where no aromaticity could have been expected.[27c] Stepwise dihydroxylations of porpholactone and bacteriodilactones provide compounds of intermediate oxidation states between the tris-diol and tris-lactone, illustrating the progression of macrocycle aromaticity with increasing number of oxazolone moieties. DFT computations of the aromaticity of these systems shed light on the origin of the aromaticity and the preferred delocalization pathways.

RESULTS AND DISCUSSION

Synthesis of Hexahydroxypyrrocorphin. The OsO_4-mediated dihydroxylation of *meso*-tetrakis(pentafluorophenyl)-porphyrin **1**^{F} using 4 equiv of OsO_4 but otherwise standard reaction conditions[3,5,6] quantitatively consumed the starting material and formed, next to the known green bacteriochlorin **3**^{F}-*Z* (in 45% yield),[5] a more polar, bright-red compound **9** (in 40% yield) (Scheme 2).

The composition of compound **9** ($C_{44}H_{17}F_{20}N_4O_6$ for M·H^+, as per by ESI^+ HR-MS) suggests the introduction of six hydroxy groups, thus supporting it being a hexahydroxylated pyrrocorphin. Accordingly, the Soret- and Q-band-like features of its UV−vis absorption spectrum are broadened, show no significant absorption past 600 nm, and have lower extinction coefficients when compared to those of typical hydroporphyrins, such as bacteriochlorin **3**^{F}-*Z* (Figure 3); the spectrum resembles that of, for example, free-base pyrrocorphin **6**.[24b]

The ^1H NMR spectrum of **9** provides further insight into its connectivity and indicates the presence of one pyrrole and three *β*,*β*′-dihydroxypyrrolidine moieties: two signals at 5.1 and 4.9 ppm with an integrated intensity ratio of 1:2 can be assigned to pyrroline hydrogens and one upfield-shifted singlet (at 6.5 ppm) to a pyrrole *β*-hydrogen atom. Two signals assigned to N−H peaks are significantly downfield-shifted (6.3 and 5.7 ppm, exchangeable with D_2O) compared to the usual position of these protons in 18 *π*-aromatic porphyrinoids (e.g., −2 ppm for the NH protons in **3**^{F}-*Z*). For a further discussion of the lack of diatropic ring current in compound **9**, see below.

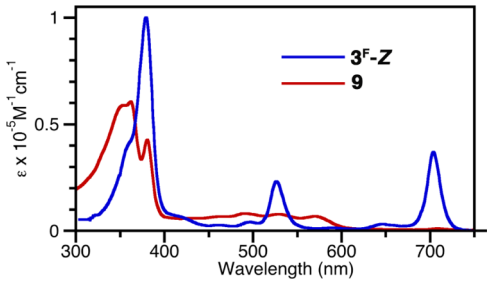

Figure 3. UV−vis spectra of hexahydroxypyrrocorphin **9** (CH_3OH) and tetrahydroxybacteriochlorin **3**^{F}-*Z* (CH_2Cl_2).

The ^1H NMR spectra of pyrrocorphin **9** match its assignment as a single diastereomer of twofold symmetry, even though multiple stereoisomers could be expected for a tris-*vic*-*cis*-dihydroxylated species. We showed previously that two *cis*-diol moieties located on opposite pyrrolines (like in **3**^{F}-*Z*) strongly prefer to be in the same hemisphere defined by the mean plane of the chromophore,[5] while those located on adjacent pyrrolines prefer to point into opposite hemispheres.[6] Others have demonstrated stereochemical effects to control the stereochemistry of cycloadditions to porphyrins.[25] Since only one twofold-symmetric isomer was found and the "down-up-down" isomer **9** shown fulfills the stereochemical requirements of both precedents, we conclude that this non-chiral isomer (a meso-compound) is formed selectively (cf. also to the selectivity revealed for the formation of **6**/**6Ni**).[24b]

Unlike *β*-unsubstituted pyrrocorphins,[18e] free-base hexahydroxypyrrocorphin **9** is chemically robust; it could be chromatographed without special precautions; no decomposition or oxidation was observed. The formation of its tautomeric porphyrinogen form was also not observed.

Synthesis of Porphotrilactones. Treatment of hexahydroxypyrrocorphin **9** under the conditions known to convert *β*,*β*′-dihydroxylated hydroporphyrins to the corresponding porpholactones (MnO_4^- in the presence of a phase-transfer cation)[6] transformed hexaol **9** in 50% isolated yield into a

https://doi.org/10.1021/acs.joc.2c01202
J. Org. Chem. 2022, 87, 12096−12108

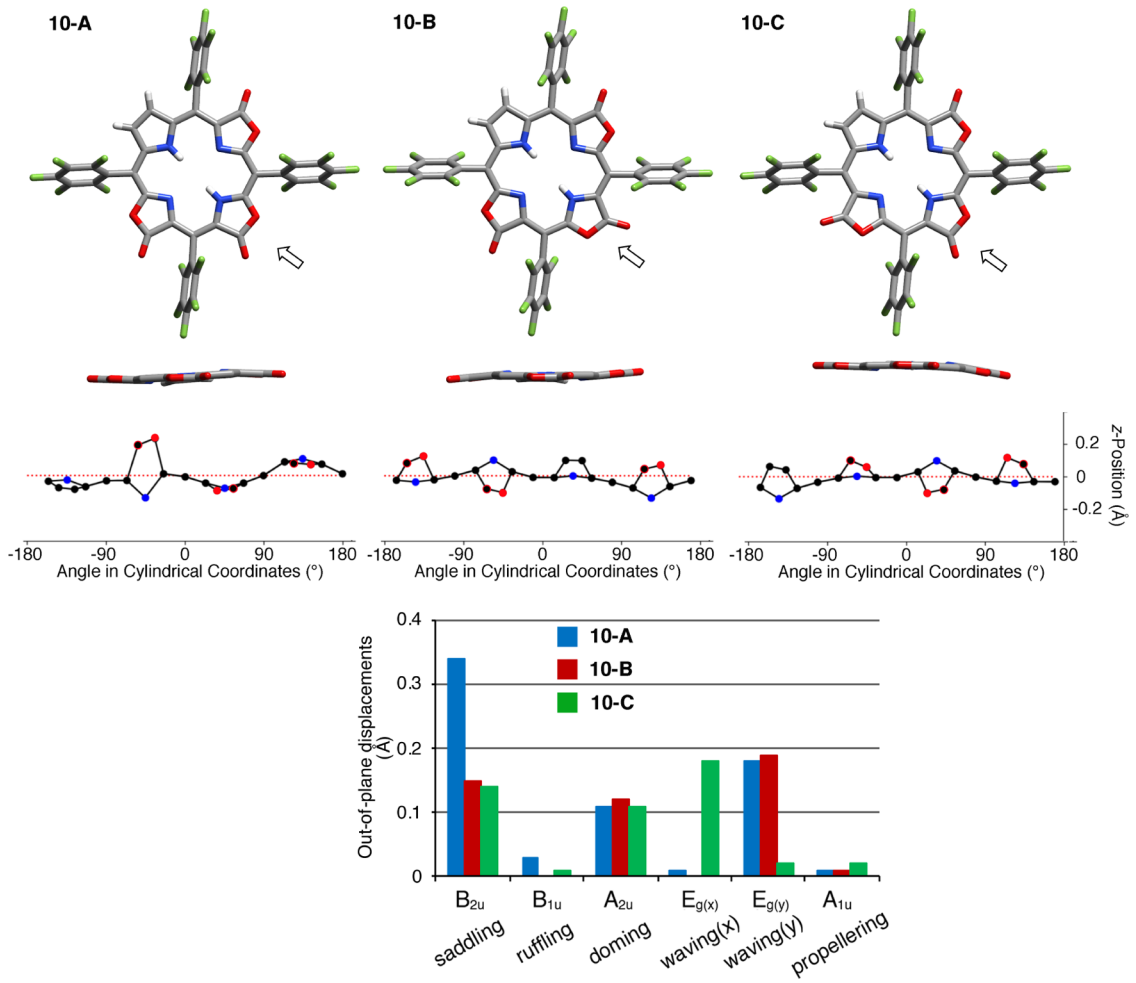

Figure 4. Stick representation of top (top row) and side (second row) views of the X-ray single-crystal structures of the pyrrocorphinotrilactone isomers **10** indicated. Arrows indicate the side view perspective. All meso-substituents are removed in the side view; all disorder and solvents are removed for clarity. The corresponding out-of-place diagrams are shown in the third row. The bar diagram shows the NSD analysis[30] of the chromophore conformations as implemented by Kingsbury and Senge.[32] For details of the structural determinations and structural analyses, see the Supporting Information.

purplish low polarity fraction, **10** (Scheme 2). However, it was found necessary to wash the crude reaction mixture with conc. TFA to be able to isolate this fraction; in the absence of this wash, only the formation of highly polar, green products was observed (see also below).

Preparative plate chromatographic separation of the purplish fraction revealed it to contain purple **10-A** as the main product and a smaller blue fraction that proved to be a 2:1 mixture of two compounds, **10-B** and **10-C**. Repeated plate chromatographic separation of the latter mixture (silica, 3:2 hexanes–CH_2Cl_2) allowed the isolation of pure isomeric forms of **10-B** (blue-colored) and **10-C** (brownish colored fraction, trace quantities).

All three compounds possess identical compositions ($C_{41}H_3F_{20}N_4O_6$, for $[M - H]^-$, as per ESI^- HR-MS), corresponding to the composition of the pyrrocorphin trilactone isomers **10**. The FT-IR spectra of **10-A** through **10-C** provided diagnostic signals in the range for the carbonyl stretching frequencies in porpholactones (see the Supporting Information for details). Four pyrrocorphintrilactone regioisomers are possible for **10**, but the presence of the fourth possible isomer **10-D** was not detected.

Ke *et al.* succeeded in the separation of the two bacterio–dilactone isomers $\mathbf{5}^{\mathbf{F}}$ by way of their zinc(II) complexes.[11a] We thus prepared the zinc complexes of the 2:1 isomeric mixture **10-B**/**10-C** and attempted their separation but found it to be equally difficult as the separation of the free bases; we thus abandoned a deeper investigation of these zinc complexes. Nonetheless, some observations on the formation and properties of the zinc complexes of the trilactones are notable. The formation of the zinc complexes of **10-A** (or the **10-B**/**10-C** mixture) required comparably harsh conditions (10 equiv $Zn(OAc)_2{\cdot}2H_2O$ in DMF at reflux temperature for 60–75 min). We have previously shown the increase in acidity and retardations of the metal ion kinetics with increasing β-oxo-substitution of the macrocycle;[28] the finding of the relative reluctance of zinc(II) to insert into the trilactones fits the pattern. The optical spectra of the zinc(II) complexes show 13–15 nm bathochromic shifts for their Soret bands upon metalation, but the position of the longest wavelength band remained essentially unchanged (see the Supporting Information). In this respect, these chromophores resemble metallobacteriochlorins.[29] The ^{1}H NMR spectrum of **10-A-Zn** is also very similar to that of the corresponding free base, except

https://doi.org/10.1021/acs.joc.2c01202
J. Org. Chem. 2022, 87, 12096–12108

for the disappearance of the inner core NH protons (see the Supporting Information).

The ^{1}H NMR spectroscopic assignment of the free-base isomers of **10** is complicated by the fact that the molecules contain only four hydrogen atoms (2 × β-H and 2 × NH). The number of carbonyl carbon peaks in the ^{13}C NMR spectrum of these compounds is also not diagnostic. Similarly, the heavily overlapping ^{19}F NMR spectra of the compounds also do not allow the assignment of the isomers (for details, see the Supporting Information). We thus relied on single-crystal X-ray crystallography for the unambiguous identification of their connectivities (Figure 4).

The crystal structures of the porpholactones are often complicated by extensive disorder.[8] Fortunately, isomer **10-A** crystallized with a simple flip disorder that allowed its unequivocal assignment. Fortuitously also, the mixture of **10-B** and **10-C** crystallized as a mixture of the two compounds in a way that also allowed their clear distinction (for details to the X-ray crystal diffractometry, see the Supporting Information). These circumstances allow their unequivocal assignment.

The chromophores of all three isomers deviate only slightly from planarity, and all show similar deformation modes. Analyzing the deformation modes of the chromophore conformations using normal-structure-deformation (NSD) analysis[30,31] as implemented by Kingsbury and Senge,[32] it can be shown that the deformations are more or less evenly spread over the saddling, doming, and waving deformation modes, with only the conformation of isomer **10-A** showing a larger (but in absolute terms still very small) saddling proportion (Figure 4). Generally, the deformations of the trilactones are similar in deformation type and extend as exhibited by the structures of the mono- and di-lactones.[6,8,11a,17c] In essence, the minor steric interaction introduced by the lactone groups[8] is small enough so not to lead to any major accumulative effects. We do not consider structural factors to be a major contributor to their differences in electronic structure.

The UV−vis absorption spectra of all three isomers of trilactones **10** are much more typically porphyrinic and red-shifted compared to the spectrum of the parent pyrrocorphin **9** (Figure 5). Notably, the spectra of the three isomers are appreciably different from each other. For instance, the spectrum of **10-C** (λ_{max} = 700 nm) is 39 nm red-shifted and endowed with a much more intense λ_{max} band compared to the spectrum of **10-B** (λ_{max} = 669 nm) and is 63 nm red-shifted with respect to the spectrum of **10-A** (λ_{max} = 637 nm). The

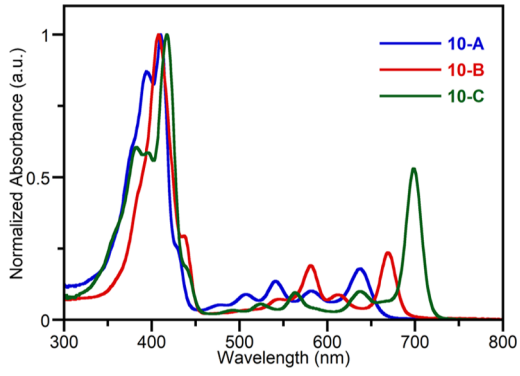

Figure 5. UV−vis spectra of trilactone isomers **10-A**, **10-B**, and **10-C** (all CH_2Cl_2).

strong regiochemical influence of the lactone moieties on the electronic structure of the chromophores was previously rationalized for the dilactone isomers;[11a,17a,b] a similar finding was also reported for β-oxoporphyrins[27c,33] or other substituents on the chlorin chromophore.[34]

The trilactones are generally stable and easy to handle, but when exposed for extended periods on silica gel (in CH_2Cl_2 with small fractions of hexanes or methanol), highly polar green compounds are formed. Similar to the polar compounds formed during their synthesis, treatment with a strong acid (TFA) recovers the trilactones. We surmise that the polar products are the hydrated forms of the trilactones. The susceptibility of the lactone moiety in the porpholactones to nucleophilic attack is very well known;[16] we surmise that the electron-poor trilactones are even more susceptible to nucleophilic attack than the monolactones. Their evaluation in chemosensing applications is ongoing.

Conjugation Pathways and Aromaticity of Hexahydroxypyrrocorphin and the Porphotrilactones. The nature of the electronic structure of the pyrrocorphin π-system in general, and how β-carbonyl functionalities affect it in particular, received only scant attention.[22,24a,25,26,35] NMR spectroscopic data and DFT calculations illuminate some fundamental questions with respect to the degree of macrocycle aromaticity (or lack thereof) of hexahydroxypyrrocorphin **9** and trilactones **10**.

A comparison of the ^{1}H NMR spectrum of the macrocycle-aromatic benchmark tetrahydroxybacteriochlorin $\mathbf{3^F}$-*Z* with that of hexahydroxypyrrocorphin **9** provides a sense for the degree of loss of diatropic ring current upon (formal) dihydroxylation of the bacteriochlorin (Figure 6). The experimental spread $\Delta\delta_{\beta\text{-NH}}$ between the chemical shifts of the inner NH protons (at −2.1 ppm) and the β-protons (at 8.3 ppm) in the aromatic bacteriochlorin $\mathbf{3^F}$-*Z* is well in excess of 10 ppm (Figure 7). In comparison, $\Delta\delta_{\beta\text{-NH}}$ of the corresponding protons in pyrrocorphin **9** is only ∼0.6 ppm (taking the average of the two non-equivalent NH protons at 6.0 ppm and the β-protons at 6.6 ppm).

This collapse of the aromatic ring current of bacteriochlorin $\mathbf{3^F}$-*Z* upon dihydroxylation can also be modeled using current density susceptibility tensor computations, as implemented in the GIMIC program (Figure 7).[36] The strong aromatic ring current in bacteriochlorin $\mathbf{3^F}$-*Z* follows the well-known outer-inner-outer-inner conjugation pathway.[2b] Upon dihydroxylation to form pyrrocorphin **9**, the ring current collapses; this pyrrocorphin chromophore is, as expected, essentially non-aromatic.

Remarkably, upon oxidation of the dihydroxypyrroline moieties, the $\Delta\delta_{\beta\text{–NH}}$ value for trilactones **10** widens to ∼3.8 ppm for **10-A** and to ∼6.9 ppm for **10-B** (or **10-C**, as seen in the ^{1}H NMR spectrum of the mixtures of the two, see the Supporting Information). The two "more aromatic" isomers **10-B**/**10-C** are also imbued with the more bathochromically shifted optical spectra (λ_{max} = 698/669 nm) when compared to that of **10-A** (λ_{max} = 638 nm), corresponding to observations made for reduced porpholactones.[17b] Thus, upon oxidation, the aromatic ring current was recovered, even though the β,β'-double bond needed for a classic description of the aromatic π-system of a hydroporphyrin was not restored. This suggests a non-classic π-conjugation pathway for the aromatic system in the porphotrilactones, perhaps similar to that of the recently described aromatic trioxopyrrocorphins.[27c,35b]

https://doi.org/10.1021/acs.joc.2c01202
J. Org. Chem. 2022, 87, 12096−12108

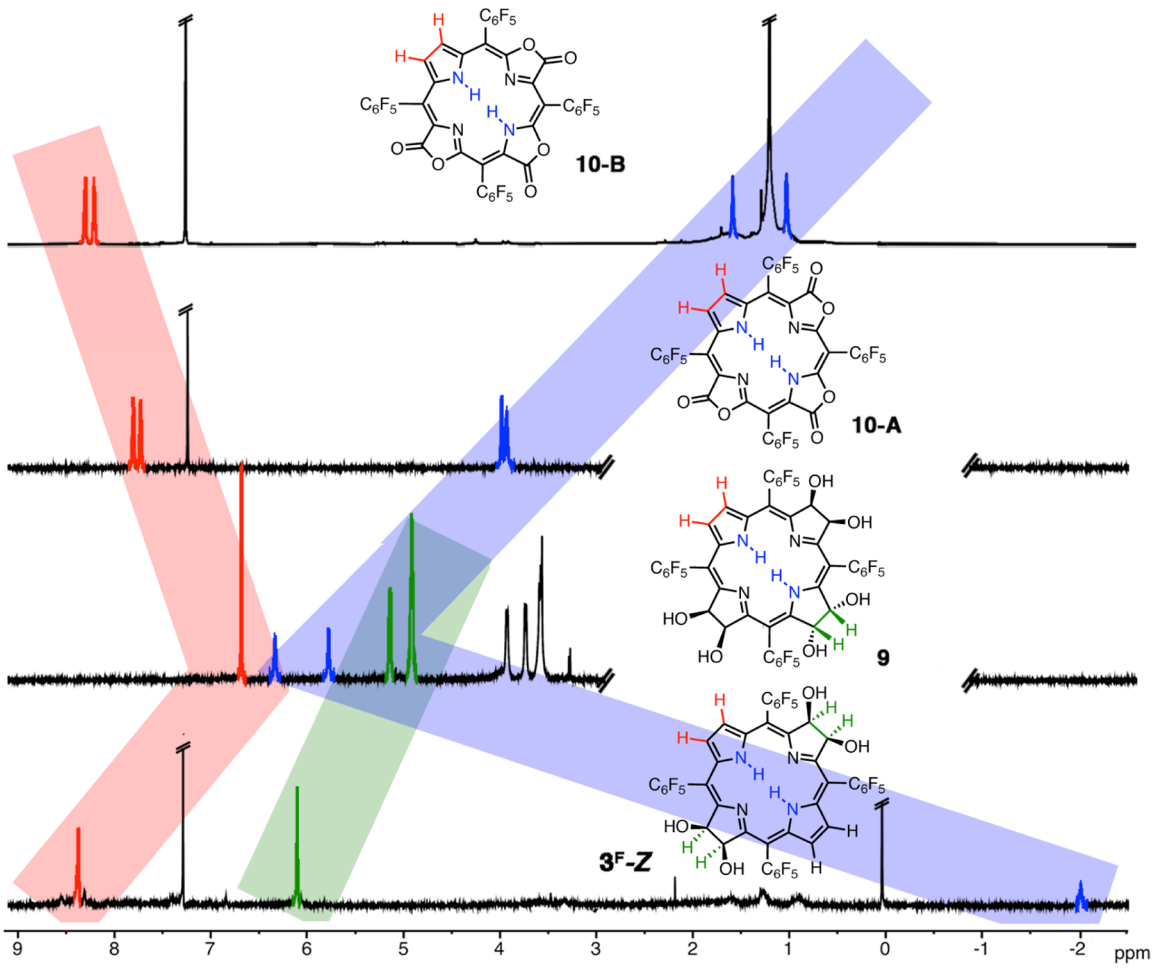

Figure 6. Comparison of the ^{1}H NMR spectra (400 MHz, 20 °C, $CDCl_3$, except for **9**, CD_3CN was used) of the compounds indicated, highlighting the trends of the shifts for the pyrroline protons (green), pyrrolic protons (red), and the NH protons (blue). For the full NMR spectra and details of the computations, see the Supporting Information.

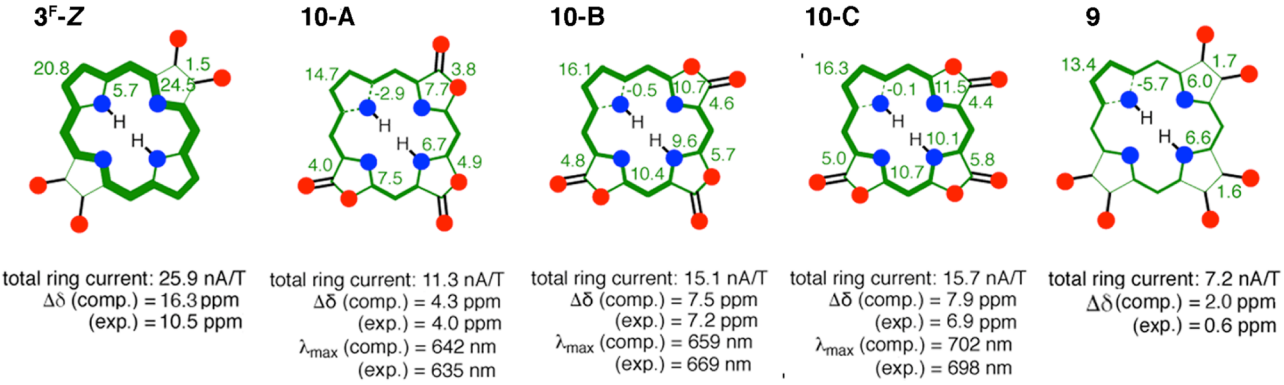

Figure 7. Visualization of the outcomes of the GIMIC ring current computations (BHandHLYP//BHandHLYP) for the compounds indicated. The relative green line thickness chosen corresponds to the computed ring current values printed next to the corresponding bonds (values in nA/T). NMR shift values used were computed at the BHandHLYP/def2TZVP//BHandHLYP/6-31G(d) level of theory, and the UV−vis spectra were recorded at the BHandHLYP level of theory. For the full NMR spectra and details to the computations, see the Supporting Information.

Even though Gouterman stated already in his 1989 paper on the discovery of the *meso*-C_6F_5-substituted porpho-mono- and -dilactones that "... it is fair to say that the oxa and oxo atoms [of porpholactone] are fully participating in the conjugation, making the ring more porphyrin-like than chlorin-like,"[9b] it is remarkable that this effect is strong enough such that the chromophores with a pyrrocorphin-type arrangement of double and single bonds around the macrocycle like **10** are nonetheless rendered aromatic.

The computed ring currents suggest an aromatic inner-inner-inner-outer conjugation pathway of a 17-membered, 18 π-electron system. How and why this conjugation pathway appears to be different from the 16-membered, 18 π-electron inner-inner-inner-inner conjugation pathway deduced for the

https://doi.org/10.1021/acs.joc.2c01202
J. Org. Chem. 2022, 87, 12096−12108

Scheme 3. Osmylation of Porpholactone 4^F and Bacteriodilactone 5^F[a]

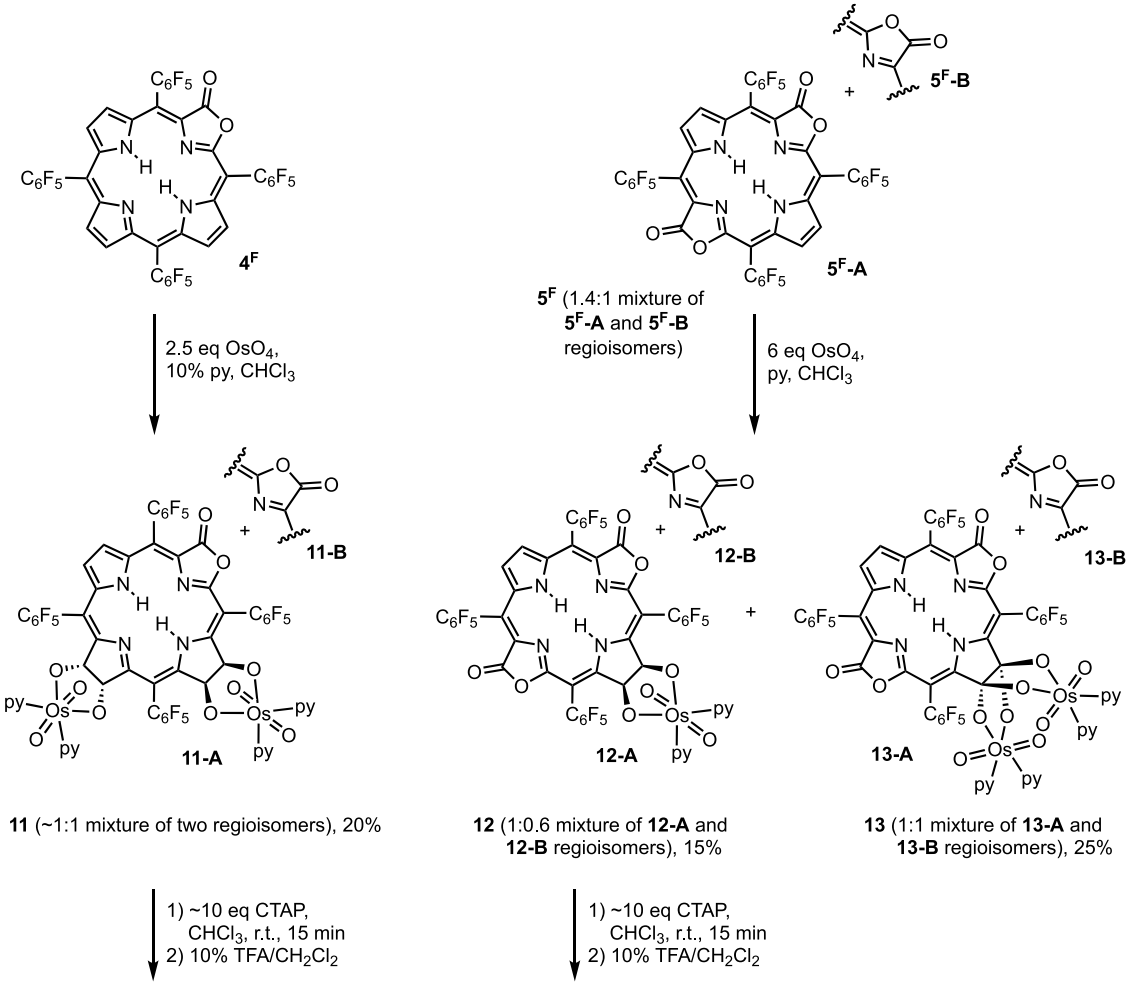

[a]py = pyridine.

octaethylpyrrocorphin triketones we described recently[27c] is not clear at this time. Unlike for the triketones, structural indications for this conjugation pathway could not be gleaned from the crystal structures of any of the three trilactone isomers.

Stepwise Syntheses of Porphotrilactones. A reduction of free-base porphomonolactone 4^F using Woolins' reagent (2,4-diphenyl-1,3-diselenadiphosphetane 2,4-diselenide) generated tetrahydroporpholactone **8**; its NMR data suggested the presence of an essentially non-aromatic pyrrocorphin (spread of NH protons and pyrrole β-protons ~0.6 ppm).[26] The cycloaddition adducts to the β,β'-position of two isomeric bacteriodilactones also showed small (and isomer-dependent) $\Delta\delta_{\beta\text{-NH}}$ spreads in their ^{1}H NMR spectra (~3.8 and ~1.2 ppm for each of the two isomers), indicative of a macrocycle with drastically reduced aromaticity.[17b] This suggests that the interaction of an increasing number of lactone moieties is needed to restore the macrocycle ring current.

We set out to systematically dehydroxylate porpholactone 4^F and bacteriodilactone 5^F with the goal of preparing mixed oxazolone-pyrroline-based chromophores that might provide deeper insight into how many oxazolones are required in tris-modified systems to support an aromatic macrocycle ring current (Scheme 3).

Reaction of porpholactone 4^F with 2.5 equiv of OsO_4 under the otherwise classic osmylation conditions ($CHCl_3$, 10% pyridine, r.t. for 24 h) resulted in the formation of bis-osmate ester **11** in 20% isolated yield, along with the mono-osmate ester of porpholactone as the major product.[8] The absorption spectrum of **11** is highly blue-shifted and less intense compared to that of the starting porphyrin-like spectrum of porpholactone 4^F (Figure 8). It resembles more conjugated oligopyrroles than macrocycle-aromatic porphyrinoids, indicative for a loss of aromatic character when compared to a porpholactone. The reaction is expected to form two regioisomers, **11-A** and **11-B**, distinguished by the relative orientation of the lactone moiety. Our previous work showed that oxidation or osmylation reactions of the porpholactones show some regioselectivity,[6] generally forming hard-to-separate or inseparable mixtures of regioisomers; we never experienced any regiospecific reaction. The case for **11** is inconclusive. Because of the paucity of proton signals that could be diagnostic (e.g., only 2 β-hydrogens are present—and their signals are unresolved), the ^{1}H and ^{19}F NMR spectra of bis-osmate ester **11** are inconclusive whether a mixture of **11-A**

https://doi.org/10.1021/acs.joc.2c01202
J. Org. Chem. 2022, 87, 12096−12108

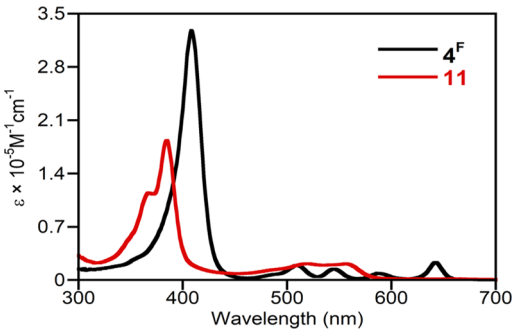

Figure 8. UV−vis spectra (CH_2Cl_2) of $\mathbf{4}^{\mathbf{F}}$ and **11-A/B**.

and **11-B** was formed (likely), or the reaction was regiospecific (unlikely) (for details, see the Supporting Information). The ^{1}H NMR spectrum allows, however, the identification of the NH signals and a determination of the average $\Delta\delta_{\beta\text{-NH}}$ value of 1.6 ppm. This value is slightly higher than found for hexahydroxypyrrocorphin **9**, but much lower than that of any of the trilactones (cf. to Figure 7). The molecule can be considered as non-macrocycle aromatic.

Reaction of bacteriodilactone $\mathbf{5}^{\mathbf{F}}$ (as a 1.4:1 mixture of regioisomers $\mathbf{5}^{\mathbf{F}}$**-A** and $\mathbf{5}^{\mathbf{F}}$**-B**) with a sixfold stoichiometric excess of OsO_4 (in $CHCl_3$ and 40% pyridine to better solubilize the dilactones) led to near-quantitative conversion of the starting material and the formation of two main products, pink product **12** and blue product **13** (Scheme 3). Despite their differing appearance on the chromatography plate or column, the UV−vis spectra of the two compounds are very similar to each other, but significantly blue-shifted, less intense, and with a broadened Soret band compared to the spectrum of the starting bacteriodilactones $\mathbf{5}^{\mathbf{F}}$ (Figure 9). We interpret this

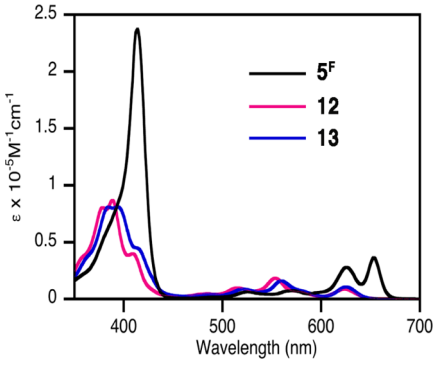

Figure 9. UV−vis spectra of $\mathbf{5}^{\mathbf{F}}$, **12**, and **13**, each as regioisomer mixtures (all CH_2Cl_2).

as the first indication for the loss of aromaticity upon osmylation. On the other hand, the Soret band extinction coefficient is significantly higher and paired with better resolved Q-bands than in hexahydroxypyrrocorphine **9** (cf. to Figure 3).

^{1}H NMR spectroscopy showed that the presence of regioisomers in the starting material was retained in the two products. This could be clearly seen, for instance, in the number and coupling patterns for the ^{1}H NMR signal attributed to the sole pyrrole-type β,β'-bond present in the products: singlet at 7.3 ppm and doublet at 7.5 ppm for the products derived from $\mathbf{5}^{\mathbf{F}}$**-A** and $\mathbf{5}^{\mathbf{F}}$**-B**, respectively. However, the original 1.4:1 isomer ratio of the starting material $\mathbf{5}^{\mathbf{F}}$ shifted to a 1:0.6 and 1:1 ratio in **12** and **13**, respectively, likely because of a minor regioselectivity for the osmylation of both isomers of $\mathbf{5}^{\mathbf{F}}$.[6]

The experimental $\Delta\delta_{\beta\text{-NH}}$ values much vary for both isomers of **12** and **13** [1.68 ppm for **12-A** and 4.26 ppm for **12-B**; 1.82 ppm for **13-A** (*cis*-isomer) and 4.36 for **13-B** (*trans*-isomer)]. The (average) values place these molecules between the starting material $\mathbf{5}^{\mathbf{F}}$ (aromatic) and the bis-osmate ester lactone **11** and hexahydroxypyrrocorphin **9** (both non-aromatic).

The presence of osmate esters in both products **12** and **13** could be deduced by ^{1}H NMR spectroscopy. The spectra showed (at 7.4−8.6 ppm) the diagnostic doublet, triplet, triplet signals in 1:2:2 ratio for the pyridines coordinated to the osmate esters. Based on ^{1}H NMR peak integration, the number of pyridines that are coordinated to the osmate esters in compound **13** is double the number observed in compound **12**. Another difference between the ^{1}H NMR spectra of **12** and **13** is that typical pyrroline protons (at 6.1 and 6.3 ppm for the two isomers) are visible in **12** but not in **13**. This suggests that compound **12** is a mono-osmate ester and **13** is the corresponding bis-osmate ester, a proposition corroborated by single-crystal X-ray diffractometry (Figure 10).

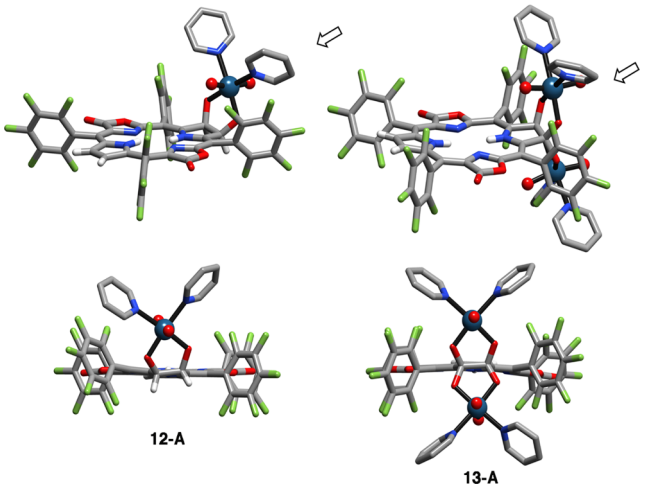

Figure 10. Stick representation of top (top row) and side (bottom row) views of the X-ray single-crystal structures of pyrrocorphinodilactone osmate ester **12-A** and pyrrocorphinodilactone bis-osmate ester **13-A**. Arrows indicate the side view perspective. Only the majority isomer is shown; all disorder, all hydrogen atoms of bonded pyridines of the osmate esters, and solvents (if present) are removed for clarity. For more information, see the Supporting Information.

The crystal structures of **12** and **13** confirm them to be osmate esters of bacteriodilactone $\mathbf{5}^{\mathbf{F}}$ and are present as mixtures of regioisomers defined by the relative orientation of the lactone moieties to each other. A careful analysis of the isomers present provides insight in some regioselectivities that controlled the reaction. While osmylation of mirror-symmetric isomer $\mathbf{5}^{\mathbf{F}}$**-A** may result in the formation of two different isomers, only isomer **12-A** resulting from the reaction of pyrrole facing the oxa-oxygen atoms was observed to form (or at least crystallized). Reaction of the minor twofold symmetric isomer $\mathbf{5}^{\mathbf{F}}$**-B** with OsO_4 also forms only one isomer, **12-B**, that is observed spectroscopically and as the minor component in the crystal. The macrocycle of products **12** is idealized planar, as was also observed for other hydroporphyrin osmate esters.[6]

https://doi.org/10.1021/acs.joc.2c01202
J. Org. Chem. 2022, 87, 12096−12108

Only a hint of a distortion in the pyrroline moieties to evade a fully eclipsed arrangement of the pyrroline hydrogen atoms is detectable.[6]

The X-ray crystal structure of **13**, as a mixture of regioisomeric products **13-A** and **13-B** that co-crystallize, confirms its bis-osmate ester connectivity, whereby both osmates are located on the same β-carbon atoms. Such double addition is generally observed by reaction of triple bonds with OsO_4.[37] This structure is the first observation of this bis-osmate motif resulting from the oxidation of a double bond we are aware of. Possibly, the pyrroline of the first adduct **12** became oxidized to a pyrrole under the harshly oxidizing conditions of the reaction and then reacted with a second equivalent of OsO_4.

Like for the other osmate esters,[6] no ionization technique could be found for either compound (ESI and MALDI were tested) that delivered mass spectra showing the parent species or readily interpretable fragment ions.

CONCLUSIONS

In conclusion, aggressive dihydroxylation of *meso*-tetrakis(pentafluorophenyl)porphyrin $\mathbf{1^F}$ provides first access to an unexpectedly robust but expectedly non-aromatic hexahydroxypyrrocorphin **9** as a single stereoisomer. Permanganate-mediated oxidation of hexaol **9** smoothly converted pyrrocorphin **9** into three out of four possible isomers of the novel and planar porphotrilactones **10**, thus replacing three ring carbon atoms by oxygen atoms and oxidizing the adjacent β-carbon atom in a one-pot process. This conversion recovers the majority of the porphyrinic aromaticity, with the trilactone regioisomers showing distinctly different degrees of aromaticity as well as different optical spectra. Experimental ^{1}H NMR and computational data were in full agreement and able to quantify the diatropic ring currents. A unique 17-membered, 18 π-electron outer-inner-inner-inner conjugation pathway was deduced for these compounds.

More generally, this work extends the breaking-and-mending approach[7b] toward pyrrole-modified porphyrins to tris-modified systems and provides further insight into the electronic structure of porphyrinoids in which β,β'-double or single bonds were replaced by lactone moieties, highlighting their unusual electronic influences on the macrocycle aromaticity. Mixed pyrrole pyrroline (2 or 1)-oxazolone (1 or 2, respectively) macrocycles formed by osmylation of porpholactone and porphodilactones. The osmylated compounds represent oxidation state intermediates between the trilactone and hexahydropyrrocorphin. This is also reflected in their intermediate aromaticity parameters.

This work expands on the knowledge of pyrrocorphins and pyrrocorphin analogues and highlights the necessity for three lactone moieties to be present to sustain a strong macrocycle-aromatic π-system in these pyrrocorphin analogues.

EXPERIMENTAL SECTION

Materials. Solvents and reagents were used as received.

Cetyltrimethylammonium MnO_4^- (CTAP) was prepared as described.[38] Porphyrin $\mathbf{1^F}$ is commercially available;[39] porpholactone $\mathbf{4^F}$ and bacteriodilactone $\mathbf{5^F}$ (as a 1.4:1 mixture of regioisomers $\mathbf{5^F}$-**A** and $\mathbf{5^F}$-**B**) were prepared as previously described.[6,8]

Aluminum-backed, silica gel 60, 250 μm thickness analytical plates and 20 × 20 cm, glass-backed, silica gel 60, 500 μm thickness preparative TLC plates and standard grade, 60 Å, 32−63 μm flash column silica gel were used. Flash column chromatography was performed manually or on an automated flash chromatography system using normal-phase silica gel columns.

CAUTION: OsO_4 is a highly toxic, volatile solid that must be handled exclusively under a well-ventilated fume hood. Particular hazards are inhalation and exposure of the eye to OsO_4 fumes. Personal protective equipment (nitrile gloves, lab coat, and safety goggles) is required. The reactions performed by us were frequently scaled such that the contents of an entire OsO_4 ampule could be used all at once; the ampule was broken open (leather gloves over the nitrile gloves), and the ampule and cap were immediately dumped into the reaction flask containing all other solvents and reactants; the empty glass ampule was retrieved by filtration or with pincers before the solvent was removed by rotary evaporation. When less than the contents of an entire OsO_4 ampule was required, OsO_4 was dissolved in distilled pyridine in a 10 or 25 mL volumetric flask; aliquots were retrieved by syringe. The flasks were well sealed, stored cold, and used up within days. Wastes that might contain unreacted OsO_4 were treated with $NaHSO_3$ before disposal.

General Procedure A for the Osmylation of Porphyrins and Porpholactones, *meso*-Tetrakis(pentafluorophenyl)-2,3-*cis*-7,8-*cis*-12,13-*cis*-hexahydroxypyrrocorphin (9). *meso*-Tetrakis(pentafluorophenyl)porphyrin ($\mathbf{1^F}$) (200 mg, 0.20 × 10^{-3} mol) was dissolved in $CHCl_3$ (20 mL) and freshly distilled pyridine (5 mL) in a 50 mL round-bottom flask equipped with a stir bar. The mixture was treated with 4 equiv of OsO_4 (0.82 × 10^{-3} mol; 5.2 mL of a stock solution of 1.0 g OsO_4 dissolved in 25 mL of pyridine) (**Caution**, see note above). The flask was stoppered, shielded from light with aluminum foil, and stirred at ambient temperature. The disappearance of the starting material/appearance of the product was monitored by TLC and UV−vis spectroscopy. Once no further progress of the reaction was detectable (24 h), approximately 50% of the solvent was removed by rotary evaporation. A saturated solution of $NaHSO_3$ in MeOH/H_2O (1:1) (30 mL) was added to the crude reaction mixture, the flask was stoppered and wrapped in aluminum foil, and the biphasic solution was vigorously stirred at ambient temperature for 24 h. Once no further progress of the reaction was detectable by TLC of the organic layer, the mixture was transferred into a 250 mL separatory funnel. After the addition of CH_2Cl_2 (~50 mL), the organic fraction was separated and filtered through a short plug of diatomaceous earth (Celite). The solvent was then removed to dryness by rotary evaporation. A gentle stream of N_2 for several hours ensured that the crude material was thoroughly dried before it was purified via flash chromatography (silica−CH_2Cl_2/1.0% MeOH). The lowest polarity material was *meso*-tetrakis(pentafluorophenyl)-2,3-*cis*-12,13-*cis*-tetrahydroxybacteriochlorin $\mathbf{3^F}$-**Z** (45% yield; 96 mg),[5] and the second major fraction was pyrrocorphin **9**, isolated in 40% (88 mg) yield as a red-color solid. **9**: R_f (2% MeOH/CH_2Cl_2) = 0.22; ^{1}H NMR (400 MHz, CD_3CN): δ 6.65 (d, J = 2.3 Hz, 2H), 6.31 (s, 1H), 5.75 (s, 1H), 5.12 (d, J = 5.7 Hz, 2H), 4.93−4.87 (overlapping d, 4H), 3.92 (d, J = 6.1 Hz, 2H), 3.73 (d, J = 6.5 Hz, 2H), 3.59 (d, J = 6.5 Hz, 2H) ppm; ^{19}F NMR (376 MHz, CD_3OD): δ −138.2 (dd, J = 23.18 Hz, 7.56 Hz, 1F), −139.9 (overlapping dd, J = 23.62, 7.33 Hz, 2F), −144.2 (dd, J = 23.35, 7.58 Hz, 1F), −158.8 (t, J = 20.01 Hz, 1F), −159.1 (t, J = 20.08 Hz, 1F), −166.1 (overlapping dd, J = 21.23, 10.70 Hz, 2F), −166.7 (overlapping dd, J = 21.23, 10.70 Hz, 2F) ppm; ^{13}C{^{1}H} NMR (101 MHz, CD_3OD): δ 171.1, 152.4, 150.3, 147.5, 147.1, 145.9, 145.1, 144.7, 143.6, 142.5, 140.0, 138.8, 136.2, 131.7, 127.4, 114.7, 114.5, 114.3, 113.5, 113.3, 113.1, 105.4, 94.2, 76.8, 73.9, 73.8, 70.9, 70.9, 70.8, 70.7, 69.9, 69.8, 69.7, 69.6 ppm; UV−vis (CH_3OH) λ_{max}, (log ε): 360.4 (4.78), 464.5 (3.84), 491.7 (3.90), 529.2 (3.84) nm; HRMS (ESI$^+$, 100% CH_3CN, TOF) m/z: $[M + H]^+$ calcd for $C_{44}H_{17}F_{20}N_4O_6$, 1077.0823; found, 1077.0780.

General Procedure B for the Oxidation of Dihydroxylated Porphyrins/Porpholactones to Form *meso*-Tetrakis(pentafluorophenyl)pyrrocorphintrilactones 10. *meso*-Tetrakis(pentafluorophenyl)hexahydroxypyrrocorphin **9** (200 mg, 1.86 × 10^{-4} mol) was dissolved in CH_2Cl_2 (50 mL) in a 50 mL round-bottom flask equipped with a stir bar. The mixture was treated with ~10 equiv of CTAP (1.0 g, 2.05 × 10^{-3} mol). The flask was stoppered, shielded from light with aluminum foil, and stirred at

https://doi.org/10.1021/acs.joc.2c01202
J. Org. Chem. 2022, 87, 12096−12108

ambient temperature. The disappearance of the starting material/appearance of the product was monitored by TLC. Upon consumption of the starting material (~15−20 min), the reaction mixture was passed through a short silica column. CH_2Cl_2 was passed through the column until the filtrate was only little colored; this fraction contains mono- and di-porpholactones (ignored here). Then, the eluent was changed to 10% CH_3OH/CH_2Cl_2 until the polar products were completely removed. The filtrates were condensed under reduced pressure. The residue was re-dissolved in 10% trifluoroacetic acid/CH_2Cl_2 (10 mL) and stirred for about 5 min (this generates/separates the trilactones from presumably manganese-containing polar precursors). Then the solvent was removed by rotary evaporation, and the residue was purified via flash chromatography (silica−CH_2Cl_2). Two fractions of trilactones were isolated: purple solid (**10-A**) (in 40% yield; 75 mg) and a 2:1 mixture of the two isomers **10-B** and **10-C** (in 10% yield; 20 mg).

Alternatively, osmate esters **11**, **12**, or **13** could be oxidized to provide essentially the same pyrrocorphintrilactone **10** isomer distribution as described for the oxidation of **9**.

*meso-Tetrakis(pentafluorophenyl)-3,7,12-trioxa-2,8,13-trioxopyrrocorphin (**10-A**).* Isolated as a purple solid. R_f (1:1, hexanes/CH_2Cl_2) = 0.53; ^{1}H NMR (400 MHz; $CDCl_3$): δ 7.82 (d, J = 2.3 Hz, 1H), 7.75 (d, J = 3.2 Hz, 1H), 4.00 (s, 1H), 3.94 (s, 1H) ppm; ^{19}F NMR (376 MHz; $CDCl_3$): δ −136.9 (d, J = 16.5 Hz, 2F), −137.9 (d, J = 11.8 Hz, 2F), −138.9 (overlapping dd, J = 23.71, 7.44 Hz, 4F), −148.6 (t, J = 20.87 Hz, 1F), −149.1 (t, J = 20.97 Hz, 1F), −149.8 (t, J = 20.85 Hz, 1F), −150.1 (t, J = 20.74 Hz, 1F), −160.01 to −160.48 (overlapping td, 8F) ppm; ^{13}C{^{1}H} NMR (101 MHz; $CDCl_3$): δ 163.2, 163.1, 162.8, 159.0, 157.3, 156.9, 148.0, 146.9, 146.6, 144.4, 144.1, 141.9, 141.4, 139.4, 137.3, 136.8, 135.1, 129.5, 128.9, 127.5, 125.3, 123.4, 122.0, 115.3, 111.2, 109.3, 109.2, 104.9, 104.7, 93.8, 29.7 ppm; UV−vis (CH_2Cl_2) λ_{max}, (log ε): 410.4 (4.95), 477.1 (3.60), 506.2 (3.88), 581.2 (3.95), 637.5 (4.22) nm; fluorescence emission ($\lambda_{excitation}$ = λ_{Soret}) (CH_2Cl_2) λ_{max}: 652 nm; Φ = 0.33; IR (neat, diamond ATR) $\nu_{C=O}$ = 1777 cm^{-1}; HRMS (ESI-, 100% CH_3CN, TOF) m/z: [M-H]$^-$ calcd for $C_{41}H_3F_{20}N_4O_6$, 1026.9733; found, 1026.9732.

*meso-Tetrakis(pentafluorophenyl)-3,8,13-trioxa-2,7,12-trioxopyrrocorphin (**10-B**).* Isolated as a blue solid from a 2:1 mixture of **10-B** and **10-C** using column chromatography with the help of UV−vis spectroscopy. R_f (1:1, hexanes/CH_2Cl_2) = 0.27; ^{1}H NMR (400 MHz; $CDCl_3$): δ 8.29 (d, J = 4.8 Hz, 1H), 8.20 (d, J = 5.7 Hz, 1H), 1.64 (s, 1H), 1.09 (s, 1H) ppm; ^{19}F NMR (376 MHz; $CDCl_3$): δ −137.09 (d, J = 13.6 Hz, 2F), −138.05 to −138.28 (m, 4F), −138.82 (d, J = 15.0 Hz, 2F), −148.71 (t, J = 21.1 Hz, 1F), −149.18 (t, J = 20.4 Hz, 1F), −149.53 (t, J = 21.1 Hz, 1F), −149.80 (t, J = 21.1 Hz, 1F), −159.76 to −159.96 (m, 2F), −160.34 (ddd, J = 64.0, 21.1, 14.3 Hz, 4F), −160.49 to −160.76 (m, 2F) ppm; ^{13}C{^{1}H} NMR (101 MHz; $CDCl_3$): δ 163.7, 162.3, 158.0, 154.9, 152.6, 146.8, 146.1, 144.3, 140.3, 139.4, 137.7, 136.8, 135.7, 127.6, 127.0, 124.5, 119.5, 118.3, 112.1, 93.7, 93.1, 31.3, 22.4 ppm; UV−vis (CH_2Cl_2) λ_{max}, (log ε): 408 (5.03), 543 (3.89), 581 (4.31), 613 (3.98), 669 (4.40) nm; fluorescence emission ($\lambda_{excitation}$ = λ_{Soret}) (CH_2Cl_2) λ_{max}: 677 nm; IR (neat, diamond ATR) $\nu_{C=O}$ = 1789 cm^{-1}; HRMS (ESI-, 100% CH_3CN, TOF) m/z: [M − H]$^-$ calcd for $C_{41}H_3F_{20}N_4O_6$, 1026.9733; found, 1026.9582.

*2:1 Mixture of meso-Tetrakis(pentafluorophenyl)-3,8,13-trioxa-2,7,12-trioxopyrrocorphin (**10-B**) and meso-Tetrakis-(pentafluorophenyl)-3,7,13-trioxa-2,8,12-trioxopyrrocorphin (**10-C**).* R_f (1:1, hexanes/CH_2Cl_2) = 0.30; ^{1}H NMR (400 MHz; $CDCl_3$): δ 8.35 (broad d, 1H (**10-C**)), 8.30 (broad d, 1H (**10-B**)), 8.28 (broad d, 1H (**10-C**)), 8.21 (s, 1H (**10-B**)), 1.45 (s, 1H (**10-C**)), 1.12 (s, 2H (**10-B**)), 1.02 (s, 1H (**10-C**)) ppm; ^{19}F NMR (376 MHz; $CDCl_3$): δ −136.95 (dd, 1F), −137.09 (dd, J = 11.04, 6.32 Hz, 3F), −138.2 (dd, J = 24.11, 6.24 Hz, 5F), −138.66 (dd, J = 22.20, 6.68 Hz, 1F), −138.83 (dd, J = 22.02, 6.44, 2F), −139.6 (dd, J = 22.00, 6.68 Hz, 1F), −148.8 (t, J = 28.04 Hz, 2F), −149.2 (t, J = 20.86 Hz, 1F), −149.5 (t, J = 20.61 Hz, 1F), −149.8 (t, J = 20.86 Hz, 2F), −159.9 (overlapping td, 3F), −160.4 (overlapping td, 6F), −160.7 (overlapping td, 3F), −161.0 (overlapping td, 1F) ppm; ^{13}C{^{1}H} NMR (101 MHz; $CDCl_3$): δ 163.7, 163.6, 162.3, 162.2, 158.0, 157.9, 157.5, 154.9, 152.6, 151.3, 146.9, 146.1, 146.0, 144.4, 140.3, 139.4, 137.8, 136.9, 136.1, 135.9, 135.7, 131.0, 130.8, 128.7, 127.7, 127.2, 127.0, 125.6, 125.3, 124.5, 123.4, 119.5, 118.4, 117.3, 112.1, 107.6, 102.5, 97.9, 93.8, 93.1, 82.4, 68.1, 38.7, 31.9, 29.7, 23.7, 14.1 ppm; UV−vis (CH_2Cl_2) λ_{max}, (log ε): 410.4 (5.37), 518.2 (4.54), 668.7 (4.60), 697.9 (4.56) nm; fluorescence emission ($\lambda_{excitation}$ = λ_{Soret}) (CH_2Cl_2) λ: 675, 706 nm; Φ = 0.28; IR (neat, diamond ATR) $\nu_{C=O}$ = 1771.11 cm^{-1}; HRMS (ESI-, 100% CH_3CN, TOF) m/z: [M + H]$^+$ calcd for $C_{41}H_5F_{20}N_4O_6$, 1028.9884; found, 1028.9896.

*[meso-Tetrakis(pentafluorophenyl)-3,7,12-trioxa-2,8,13-trioxopyrrocorphinato]zinc(II) (**10-A-Zn**).* Free-base pyrrocorphin-trilactone **10-A** (25 mg, 2.43 × 10^{-5} mol) and $Zn(OAc)_2{\cdot}2H_2O$ (54 mg, 2.43 × 10^{-4} mol, 10 equiv) were dissolved in DMF (8−10 mL) and heated to reflux until the reaction was completed (60−75 min; monitored by UV−vis spectroscopy). After completion, the reaction mixture was allowed to cool to room temperature and then deionized water (~50 mL) was added to precipitate the crude product that was retrieved by microfiltration, followed by drying under vacuum. The compound was purified by column chromatography (silica−CH_2Cl_2/1.0% acetone) to yield **10-A-Zn** as a bluish-green solid in 89% yield (24 mg); R_f (2% acetone/CH_2Cl_2) = 0.74; ^{1}H NMR (400 MHz, $CDCl_3$): δ 8.02 (d, J = 4.5 Hz, 1H), 7.95 (d, J = 4.5 Hz, 1H) ppm; ^{19}F NMR (376 MHz, $CDCl_3$): δ −137.33 (d, J = 16.3 Hz, 2F), −138.50 (d, J = 17.7 Hz, 2F), −139.21 (dd, J = 42.2, 16.3 Hz, 4F), −150.00 (q, J = 19.8, 19.1 Hz, 2F), −150.51 to −150.79 (m, 2F), −160.56 (dt, J = 23.2, 11.6 Hz, 2F), −160.87 (dq, J = 23.2, 11.6, 8.2 Hz, 6F) ppm; ^{13}C{^{1}H} NMR (101 MHz, $CDCl_3$): δ 162.8, 162.7, 161.9, 156.9, 156.4, 154.4, 147.9, 147.0, 146.6, 145.8, 144.5, 144.2, 139.3, 139.2, 136.8, 136.7, 133.6, 128.7, 127.3, 123.3, 121.0, 114.4, 111.2, 89.8, 85.1, 29.71, 23.49, 16.83 ppm; UV−vis (CH_2Cl_2) λ_{max}, (log ε): 423 (5.07), 534 (3.67), 578 (4.06), 637 (4.40) nm; fluorescence emission ($\lambda_{excitation}$ = λ_{Soret}) (CH_2Cl_2) λ_{max}: 649 nm; IR (neat, diamond ATR) $\nu_{C=O}$ = 1776, 1744 cm^{-1}; HRMS (ESI$^+$, 100% CH_3CN, TOF) m/z: [M]$^+$ calcd for $C_{41}H_2F_{20}N_4O_6Zn$, 1089.8946; found, 1089.8937.

*meso-Tetrakis(pentafluorophenyl)-tetrahydroxypyrrocorphinlactone Bis-osmate Ester **11** [1:1 Mixture of the Regioisomers meso-Tetrakis(pentafluorophenyl)-3-oxa-2-oxo-7,8-cis-12,13-cis-tetrahydroxypyrrocorphin Bis-osmate Ester (**11-A**) and meso-Tetrakis(pentafluorophenyl)-2-oxa-3-oxo-7,8-cis-12,13-cis-tetrahydroxypyrrocorphin Bis-osmate Ester (**11-B**)].* Prepared according to general procedure A by osmylation of porpholactone **4**^{F} (50.0 mg, 5.03 × 10^{-5} mol) in $CHCl_3$ (12 mL) and freshly distilled pyridine (2 mL) in a 50 mL round-bottom flask treated with 2.5 equiv of OsO_4 (1.26 × 10^{-4} mol; 0.8 mL of a stock solution of 1.0 g OsO_4 dissolved in 25 mL of pyridine). Purification via automated flash chromatography (silica cartridge−CH_2Cl_2/1.5% MeOH). The lowest polarity material **11** (1:1 regioisomeric mixture) was isolated in overall 20% (18 mg) yield as a brick-red solid. R_f (2% methanol/CH_2Cl_2) = 0.23; ^{1}H NMR (400 MHz; $CDCl_3$): δ 8.70 (d, J = 5.4 Hz, 2H), 8.65 (d, J = 5.1 Hz, 2H), 8.59 (d, J = 5.2 Hz, 2H), 8.55 (d, J = 5.1 Hz, 2H), 7.96−7.82 (m, 4H), 7.50 (t, J = 6.2 Hz, 4H), 7.42 (dt, J = 13.9, 7.1 Hz, 4H), 7.14 (d, J = 4.2 Hz, 1H), 6.77 (d, J = 2.2 Hz, 1H), 6.01 (d, J = 6.8 Hz, 1H), 5.96 (d, J = 5.0 Hz, 1H), 5.80 (d, J = 6.9 Hz, 1H), 5.78−5.73 (m, 2H), 5.15 (s, 1H). ^{19}F NMR (376 MHz; $CDCl_3$): δ −135.15 (overlapping td, J = 27.2, 26.2, 8.2 Hz, 2F), −136.58 (overlapping dd, J = 24.2, 7.8 Hz, 1F), −137.92 (dd, J = 24.5, 7.5 Hz, 1F), −139.49 (dd, J = 23.2, 8.2 Hz, 1F), −139.72 (dd, J = 23.8, 8.9 Hz, 1F), −140.32 (dd, J = 23.8, 8.2 Hz, 1F), −140.65 (dd, J = 24.5, 8.9 Hz, 1F), −153.23 (t, J = 21.1 Hz, 1F), −154.54 (td, J = 20.8, 8.5 Hz, 2F), −155.33 (t, J = 21.1 Hz, 1F), −161.99 to −162.79 (m, 4F), −163.44 to −163.97 (m, 2F), −164.33 (dt, J = 74.9, 21.1 Hz, 2F). ^{13}C{^{1}H} NMR (101 MHz; $CDCl_3$): δ 174.7, 165.0, 158.6, 156.6, 154.6, 152.3, 149.6, 149.4, 141.0, 140.8, 140.6, 140.5, 138.7, 138.4, 137.4, 136.2, 135.9, 131.1, 127.7, 125.4, 125.3, 125.2, 125.1, 123.9, 121.1, 115.8, 113.9, 112.2, 110.9, 110.1, 104.0, 96.0, 95.7, 91.9, 91.3, 90.9, 84.7 ppm; UV−vis (CH_2Cl_2) λ_{max}, (log ε): 367 (5.06), 384 (5.26), 519 (4.34), 558 (4.33) nm; IR (neat, diamond ATR) $\nu_{C=O}$ = 1764 cm^{-1}; like all hydroporphyrin osmate esters, no molecular peak

https://doi.org/10.1021/acs.joc.2c01202
J. Org. Chem. 2022, 87, 12096−12108

could be detected in the ESI^+ or ESI^- MS (100% CH_3CN, 5−30 V cone voltage).

meso-Tetrakis(pentafluorophenyl)-dihydroxypyrrocorphindilactone Osmate Ester ***12*** *and meso-Tetrakis(pentafluorophenyl)tetrahydroxypyrrocorphindilactone Bisosmate Ester* ***13***. Prepared according to the general procedure by the oxidation of bacteriodilactone $\mathbf{S^F}$ (50.0 mg, 4.95×10^{-5} mol) in $CHCl_3$ (12 mL) and freshly distilled pyridine (2 mL) in a 50 mL round-bottom flask and 5 equiv of OsO_4 (2.50×10^{-4} mol; 6 mL of a stock solution of 1.0 g OsO_4 dissolved in 25 mL of pyridine). Purification via automated flash chromatography (silica cartridge−CH_2Cl_2/1.0% MeOH). The lowest polarity material **12** (1:0.6 mixture of *cis*/*trans* isomers) was isolated in 16−20% (11−14 mg) yield as a pink-colored solid, and **13** (1:1 mixture of isomers) was isolated in 21−25% (19−23 mg) yield as a blue-colored solid. **1:0.6 Mixture of*meso*-tetrakis(pentafluorophenyl)-3,12-dioxa-2,12-dioxo-7,8-*cis*-dihydroxypyrrocorphin osmate ester (12A) and*meso*-tetrakis(pentafluorophenyl)-2,12-dioxa-3,12-dioxo-7,8-*cis*-dihydroxypyrrocorphin osmate ester (12B). 12** (1:0.6 mixture of **12-A** and **12-B** isomers): isolated as a pink-colored crystalline solid (16%; 11 mg yield). R_f (5% methanol/CH_2Cl_2) = 0.89; ^{1}H NMR (400 MHz, $CDCl_3$): δ 8.61 (d, J = 5.3 Hz, 4H (**12-B**)), 8.59 (d, J = 5.2 Hz, 2H (**12-A**)), 8.00 to 7.97 (overlapping t, 3H (**12-A** and **12-B**)), 7.68 (d, J = 1.7 Hz, 1H (**12-B**)), 7.64 (t, J = 0.7 Hz, 1H (**12-B**)), 7.50 (overlapping dt, J = 12.6, 6.5 Hz, 6H (**12-A** and **12-B**)), 7.30 (d, J = 2.0 Hz, 2H (**12-A**)), 6.37 (d, J = 6.9 Hz, 1H (**12-B**)), 6.31 (d, J = 6.9 Hz, 1H, (**12-B**)), 6.14 (s, 1H (**12-A**)), 6.12 (s, 2H, (**12-A**)), 5.14 (s, 1H, (**12-A**)), 3.69 (s, 1H, (**12-B**)), 3.13 (s, 1H, (**12-B**)) ppm; ^{19}F NMR (376 MHz; $CDCl_3$): δ −135.42 (dd, J = 24.10, 6.59 Hz, 1F (**12-B**)), −135.55 (dd, J = 24.10, 6.59 Hz, 2F (**12-A**)), −136.28 (dd, J = 24.10, 6.59 Hz, 1F, (**12-B**)), −136.92 (dd, J = 24.10, 6.59 Hz, 1F, (**12-B**)), −137.33 to −137.44 (overlapping dd, J = 24.10, 6.59 Hz, 2F (**12-B**)), −139.10 to −139.20 (overlapping dd, J = 24.10, 6.59 Hz, 2F (**12-B**)), −139.29 (overlapping dd, J = 22.96, 7.76 Hz, 4F (**12-A**)), −139.75 (overlapping dd, J = 23.71, 6.90 Hz, 2F (**12-A**)), −139.94 (dd, J = 23.79, 6.86 Hz, 1F (**12-B**)), −140.3 (dd, J = 23.80, 7.04 Hz, 1F (**12-B**)), −151.0 (t, J = 20.93 Hz, 1F (**12-B**)), −151.55 to −151.84 (m, 2F (**12-A**) & 1F (**12-B**)), −152.86 (t, J = 20.99 Hz, 2F (**12-A**)), −153.16 (t, J = 21.04 Hz, 1F (**12-B**)), −160.67 to −160.96 (overlapping td, J = 22.45, 11.04 Hz, 2F (**12-B**)), −161.06 to −161.74 (overlapping td, J = 21.96, 7.24 Hz, 6F (**12-A**)), −162.10 (td, J = 22.31, 6.74 Hz, 1F (**12-B**)), −163.10 (td, J = 21.44, 7.18 Hz, 2F (**12-A**)), −163.16 (d, J = 24.15, 8.20 Hz, 1F (**12-B**)) −163.71 to −164.03 (m, 2F (**12-B**)) ppm; ^{13}C{^{1}H} NMR (101 MHz; $CDCl_3$): δ 164.7, 164.2, 162.8, 159.1, 156.5, 154.8, 154.4, 151.1, 149.8, 147.8, 146.7, 145.4, 144.1, 141.4, 141.3, 139.3, 136.8, 134.9, 134.4, 128.1, 126.9, 126.5, 125.7, 122.9, 121.7, 121.5, 112.1, 92.2, 91.6, 86.4, 29.8 ppm; UV−vis (CH_2Cl_2) λ_{max} (log ε): 388.9 (4.94), 485.2 (3.62), 514.8 (3.99), 553.7 (4.27), 579.6 (3.78), 624.1 (3.95) nm; fluorescence emission ($\lambda_{excitation}$ = λ_{Soret}) (CH_2Cl_2) λ_{max}: 561, 605, 637 nm; Φ = 0.04; IR (neat, diamond ATR) $\nu_{C=O}$ = 1768 cm^{-1}; like all hydroporphyrin osmate esters, no molecular peak could be detected in the ESI^+ or ESI^- MS (100% CH_3CN, 5−30 V cone voltage). **1:1 Mixture of*meso*-tetrakis(pentafluorophenyl)-3,12-dioxa-2,13-dioxo-7,7,8,8-bis(*cis*-dihydroxy)pyrrocorphin bisosmate ester (13-A) and*meso*-tetrakis(pentafluorophenyl)-2,12-dioxa-3,13-dioxo-7,7,8,8-bis(*cis*-dihydroxy)pyrrocorphin bisosmate ester (13-B).** (*cis*/*trans* (1:1) mixture of isomers): isolated as blue-colored powder (25%; 23 mg yield). R_f (5% methanol/CH_2Cl_2) = 0.48; ^{1}H NMR (400 MHz; $CDCl_3$): δ 8.79−8.75 (overlapping d, J = 8.75 Hz, 8H (**13-A** and **13-B**), 7.91−7.86 (overlapping t, J = 7.38 Hz, 4H (**13-A** and **13-B**)), 7.66 (d, J = 4.40 Hz, 1H (**13-B**)), 7.45 (d, J = 4.40 Hz, 1H (**13-B**)), 7.47−7.42 (overlapping td, J = 6.37, 1.90 Hz, 8H (**13-A** and **13-B**)), 7.29 (d, J = 2.30 Hz, 2H, (**13-A**)), 5.95 (s, 1H (**13-A**)), 5.00 (s, 1H (**13-A**)), 3.55 (s, 1H (**13-B**)), 3.08 (s, 1H (**13-B**)) ppm; ^{19}F NMR (376 MHz; $CDCl_3$): δ −134.97 (d, J = 23.2 Hz, 2F), −135.06 to −135.29 (m, 4F), −135.71 (d, J = 24.5 Hz, 2F), −137.39 (d, J = 24.5 Hz, 2F), −139.09 to −139.34 (m, 6F), −151.74 (t, J = 21.8 Hz, 1F), −152.20 to −152.39 (m, 3F), −154.68 (t, J = 20.4 Hz, 3F), −155.21 (t, J = 21.8 Hz, 1F), −161.26 (t, J = 18.4 Hz, 2F), −161.50 to −161.94 (m, 6F), −165.18 to −165.57 (m, 6F), −166.02 (t, J = 19.1 Hz, 2F). ppm; ^{13}C{^{1}H} NMR (101 MHz; $CDCl_3$): δ 165.2, 164.8, 163.3, 159.8, 157.6, 154.6, 153.0, 151.9, 150.9, 150.5, 150.1, 149.9, 147.9, 146.8, 145.4, 144.2, 142.5, 141.1, 139.3, 138.2, 136.8, 135.8, 134.7, 134.2, 133.9, 131.4, 131.3, 130.8, 128.3, 126.8, 125.3, 122.4, 121.1, 120.8, 110.7, 109.6 ppm; UV−vis (CH_2Cl_2) λ_{max} (log ε): 385.6 (4.91), 486.1 (3.62), 520.1 (3.95), 560.6 (4.20), 625.4 (4.0) nm; IR (neat, diamond ATR) $\nu_{C=O}$ = 1770 cm^{-1}; like all hydroporphyrin osmate esters, no molecular peak could be detected in the ESI^+ or ESI^- MS (100% CH_3CN, 5−30 V cone voltage).

■ ASSOCIATED CONTENT

Supporting Information

The Supporting Information is available free of charge at https://pubs.acs.org/doi/10.1021/acs.joc.2c01202.

Experimental procedures and spectroscopic data of all new compounds, reproductions of select spectra, and details to the computations and X-ray diffractometry (PDF)

Accession Codes

CCDC 2017178−2017179 and 2155695−2155696 contain the supplementary crystallographic data for this paper. These data can be obtained free of charge via www.ccdc.cam.ac.uk/data_request/cif, or by emailing data_request@ccdc.cam.ac.uk, or by contacting The Cambridge Crystallographic Data Centre, 12 Union Road, Cambridge CB2 1EZ, UK; fax: +44 1223 336033.

■ AUTHOR INFORMATION

Corresponding Author

Christian Brückner − *Department of Chemistry, University of Connecticut, Storrs, Connecticut 06269-3060, United States;* orcid.org/0000-0002-1560-7345; Email: c.bruckner@uconn.edu

Authors

Nisansala Hewage − *Department of Chemistry, University of Connecticut, Storrs, Connecticut 06269-3060, United States*

Matthew J. Guberman-Pfeffer − *Department of Chemistry, University of Connecticut, Storrs, Connecticut 06269-3060, United States;* orcid.org/0000-0002-1143-0693

Nivedita Chaudhri − *Department of Chemistry, University of Connecticut, Storrs, Connecticut 06269-3060, United States;* orcid.org/0000-0001-9604-606X

Matthias Zeller − *Department of Chemistry, Purdue University, West Lafayette, Indiana 47907-2084, United States;* orcid.org/0000-0002-3305-852X

José A. Gascón − *Department of Chemistry, University of Connecticut, Storrs, Connecticut 06269-3060, United States;* orcid.org/0000-0002-4176-9030

Complete contact information is available at: https://pubs.acs.org/10.1021/acs.joc.2c01202

Notes

The authors declare no competing financial interest.

Oxazolochlorins. 22. Oxazolochlorins 21: Most Efficient Access to *meso*-Tetraphenyl- and *meso*-Tetrakis-(pentafluorophenyl)-porpholactones, and their Zinc(II) and Platinum(II) Complexes' *Molecules* **2020**, *25*, 4351.

■ ACKNOWLEDGMENTS

This contribution is dedicated to the memory of Martin Gouterman. This work was supported by the US National Science Foundation under Grant Numbers CHE-1465133 and CHE-1800361 (to C.B.) and CHE-0754580 (to J.A.G.) and a graduate fellowship DGE-1247393 (to M.J.G.-P.). The X-ray diffractometer was funded by NSF Grant CHE-1625543. We thank Victor Nemykin for assistance with MALDI mass spectrometry.

■ REFERENCES

(1) (a) Flitsch, W. Hydrogenated Porphyrin Derivatives: Hydroporphyrins. *Adv. Heterocycl. Chem.* **1988**, *43*, 73−126. (b) Montforts, F.-P.; Gerlach, B.; Hoeper, F. Discovery and Synthesis of Less Common Natural Hydroporphyrins. *Chem. Rev.* **1994**, *94*, 327−347. (c) Brückner, C.; Samankumara, L.; Ogikubo, J. *Handbook of Porphyrin Science*; Kadish, K. M., Smith, K. M., Guilard, R., Eds.; World Scientific: River Edge, NY, 2012; Vol. *17*, pp 1−112. (d) Taniguchi, M.; Lindsey, J. S. Synthetic Chlorins, Possible Surrogates for Chlorophylls, Prepared by Derivatization of Porphyrins. *Chem. Rev.* **2017**, *117*, 344−535.

(2) (a) Gouterman, M. *The Porphyrins*; Dolphin, D., Ed.; Academic Press: New York, 1978; Vol. *3*, pp 1−165. (b) Stępień, M.; Latos-Grazynski, L. Aromaticity and Tautomerism in Porphyrins and Porphyrinoids. *Top. Heterocycl. Chem.* **2009**, *19*, 83−153. (c) Otero, N.; Fias, S.; Radenković, S.; Bultinck, P.; Graña, A. M.; Mandado, M. How Does Aromaticity Rule the Thermodynamic Stability of Hydroporphyrins? *Chem.—Eur. J.* **2011**, *17*, 3274−3286.

(3) Hyland, M. A.; Morton, M. D.; Brückner, C. *meso*-Tetra(pentafluorophenyl)porphyrin-derived Chromene-annulated Chlorins. *J. Org. Chem.* **2012**, *77*, 3038−3048.

(4) Bruhn, T.; Brückner, C. Origin of the Regioselective Reduction of Chlorins. *J. Org. Chem.* **2015**, *80*, 4861−4868.

(5) Hyland, M. A.; Hewage, N.; Panther, K.; Nimthong-Roldán, A.; Zeller, M.; Samaraweera, M.; Gascon, J. A.; Brückner, C. Chromene-Annulated Bacteriochlorins. *J. Org. Chem.* **2016**, *81*, 3603−3618.

(6) Hewage, N.; Daddario, P.; Lau, K. S. F.; Guberman-Pfeffer, M. J.; Gascón, J. A.; Zeller, M.; Lee, C. O.; Khalil, G. E.; Gouterman, M.; Brückner, C. Bacterio- and Isobacteriodilactones by Stepwise or Direct Oxidations of *meso*-Tetrakis(pentafluorophenyl)porphyrin. *J. Org. Chem.* **2019**, *84*, 239−256.

(7) (a) Arnold, L.; Müllen, K. Modifying the Porphyrin Core—a Chemist's Jigsaw. *J. Porphyrins Phthalocyanines* **2011**, *15*, 757−779. (b) Brückner, C. The Breaking and Mending of *meso*-Tetraarylporphyrins: Transmuting the Pyrrolic Building Blocks. *Acc. Chem. Res.* **2016**, *49*, 1080−1092. (c) Costa, L. D.; Costa, J. I.; Tomé, A. C. Porphyrin Macrocycle Modification: Pyrrole Ring-Contracted or -Expanded Porphyrinoids. *Molecules* **2016**, *21*, 320.

(8) Brückner, C.; Ogikubo, J.; McCarthy, J. R.; Akhigbe, J.; Hyland, M. A.; Daddario, P.; Worlinsky, J. L.; Zeller, M.; Engle, J. T.; Ziegler, C. J.; Ranaghan, M. J.; Sandberg, M. N.; Birge, R. R. *meso*-Arylporpholactones and Their Reduction Products. *J. Org. Chem.* **2012**, *77*, 6480−6494.

(9) (a) Crossley, M. J.; King, L. G. Novel Heterocyclic Systems from Selective Oxidation at the β-Pyrrolic Position of Porphyrins. *J. Chem. Soc., Chem. Commun.* **1984**, 920−922. (b) Gouterman, M.; Hall, R. J.; Khalil, G. E.; Martin, P. C.; Shankland, E. G.; Cerny, R. L. Tetrakis(pentafluorophenyl)porpholactone. *J. Am. Chem. Soc.* **1989**, *111*, 3702−3707. (c) Yu, Y.; Lv, H.; Ke, X.; Yang, B.; Zhang, J.-L. Ruthenium-Catalyzed Oxidation of the Porphyrin β−β′-Pyrrolic Ring: A General and Efficient Approach to Porpholactones. *Adv. Synth. Catal.* **2012**, *354*, 3509−3516.

(10) (a) Çetin, A.; Ziegler, C. J. Structure and Catalytic Activity of a Manganese(III) Tetraphenylporpholactone. *Dalton Trans.* **2005**, 25−26. (b) Wang, X.; Nurttila, S.; Dzik, I.; Becker, R.; Rodgers, J.; Reek, N. H. Tuning the Porphyrin Building Block in Self-Assembled Cages for Branched-Selective Hydroformylation of Propene. *Chem.—Eur. J.* **2017**, *23*, 14769−14777. (c) Liang, L.; Lv, H.; Yu, Y.; Wang, P.; Zhang, J.-L. Iron(III) Tetrakis(pentafluorophenyl)porpholactone Catalyzes Nitrogen Atom Transfer to C=C and C-H Bonds with Organic Azides. *Dalton Trans.* **2012**, *41*, 1457−1460. (d) Rahimi, R.; Tehrani, A. A.; Fard, M. A.; Sadegh, B. M. M.; Khavasi, H. R. First Catalytic Application of Metal Complexes of Porpholactone and Dihydroxychlorin in the Sulfoxidation Reaction. *Catal. Commun.* **2009**, *11*, 232−235. (e) Wu, Z.-Y.; Wang, T.; Meng, Y.-S.; Rao, Y.; Wang, B.-W.; Zheng, J.; Gao, S.; Zhang, J.-L. Enhancing the Reactivity of Nickel(II) in Hydrogen Evolution Reactions (HERS) by β-Hydrogenation of Porphyrinoid Ligands. *Chem. Sci.* **2017**, *8*, 5953−5961. (f) To, W.-P.; Liu, Y.; Lau, T.-C.; Che, C.-M. A Robust Palladium(II)−Porphyrin Complex as Catalyst for Visible Light Induced Oxidative C−H Functionalization. *Chem.—Eur. J.* **2013**, *19*, 5654−5664.

(11) (a) Ke, X.-S.; Chang, Y.; Chen, J.-Z.; Tian, J.; Mack, J.; Cheng, X.; Shen, Z.; Zhang, J.-L. Porphodilactones as Synthetic Chlorophylls: Relative Orientation of β-Substituents on a Pyrrolic Ring Tunes NIR Absorption. *J. Am. Chem. Soc.* **2014**, *136*, 9598−9607. (b) Jayaraj, K.; Gold, A.; Austin, R. N.; Ball, L. M.; Terner, J.; Mandon, D.; Weiss, R.; Fischer, J.; DeCian, A.; Bill, E.; Müther, M.; Schünemann, V.; Trautwein, A. X. Compound I and Compound Ii Analogues from Porpholactones. *Inorg. Chem.* **1997**, *36*, 4555−4566.

(12) Ke, X. S.; Yang, B. Y.; Cheng, X.; Chan, L. F.; Zhang, J. L. Ytterbium(III) Porpholactones: β-Lactonization of Porphyrin Ligands Enhances Sensitization Efficiency of Lanthanide near-Infrared Luminescence. *Chem.—Eur. J.* **2014**, *20*, 4324−4333.

(13) Tang, J.; Chen, J.-J.; Jing, J.; Chen, J.-Z.; Lv, H.; Yu, Y.; Xu, P.; Zhang, J.-L. β-Lactonization of Fluorinated Porphyrin Enhances LDL Binding Affinity, Cellular Uptake with Selective Intracellular Localization. *Chem. Sci.* **2014**, *5*, 558−566.

(14) Yang, Z.-S.; Yao, Y.; Sedgwick, A. C.; Li, C.; Xia, Y.; Wang, Y.; Kang, L.; Su, B.-W.; Wang, H.; Gao, S.; Sessler, J. L.; Zhang, J.-L. Rational Design of an "All-in-One" Phototheranostic. *Chem. Sci.* **2020**, *11*, 8204−8213.

(15) (a) Khalil, G. E.; Costin, C.; Crafton, J.; Jones, G.; Grenoble, S.; Gouterman, M.; Callis, J. B.; Dalton, L. R. Dual-Luminophor Pressure-Sensitive Paint I. Ratio of Reference to Sensor Giving a Small Temperature Dependency. *Sens. Actuators, B* **2004**, *97*, 13−21. (b) Zelelow, B.; Khalil, G. E.; Phelan, G.; Carlson, B.; Gouterman, M.; Callis, J. B.; Dalton, L. R. Dual Luminophor Pressure Sensitive Paint II. Lifetime Based Measurement of Pressure and Temperature. *Sens. Actuators, B* **2003**, *96*, 304−314. (c) Gouterman, M.; Callis, J.; Dalton, L.; Khalil, G.; Mébarki, Y.; Cooper, K. R.; Grenier, M. Dual Luminophor Pressure-Sensitive Paint: III. Application to Automotive Model Testing. *Meas. Sci. Technol.* **2004**, *15*, 1986−1994.

(16) Liu, E.; Ghandehari, M.; Brückner, C.; Khalil, G.; Worlinsky, J.; Jin, W.; Sidelev, A.; Hyland, M. A. Mapping High pH Levels in Hydrated Calcium Silicates. *Cement Concr. Res.* **2017**, *95*, 232−239.

(17) (a) Guberman-Pfeffer, M. J.; Lalisse, R. F.; Hewage, N.; Brückner, C.; Gascón, J. A. Origins of the Electronic Modulations of Bacterio- and Isobacteriodilactone Regioisomers. *J. Phys. Chem. A* **2019**, *123*, 7470−7485. (b) Yao, Y.; Rao, Y.; Liu, Y.; Jiang, L.; Xiong, J.; Fan, Y. J.; Shen, Z.; Sessler, J. L.; Zhang, J. L. Aromaticity Versus Regioisomeric Effect of β-Substituents in Porphyrinoids. *Phys. Chem. Chem. Phys.* **2019**, *21*, 10152−10162. (c) Ning, Y.; Jin, G.-Q.; Zhang, J.-L. Porpholactone Chemistry: An Emerging Approach to Bioinspired Photosensitizers with Tunable near-Infrared Photophysical Properties. *Acc. Chem. Res.* **2019**, *52*, 2620−2633.

(18) (a) Johansen, J. E.; Piermattie, V.; Angst, C.; Diener, E.; Kratky, C.; Eschenmoser, A. Interconversion of the Chromophore Systems of Porphyrinogen and 2,3,7,8,12,13-Hexahydroporphyrin. *Angew. Chem., Int. Ed. Engl.* **1981**, *20*, 261−263. (b) Waditschatka, R.; Eschenmoser, A. Chemistry of Pyrrocorphins: Stereoselectivity During Porphyrinogen - Pyrrocorphin Tautomerism. *Angew. Chem., Int. Ed.* **1983**, *22*, 630−631. (c) Eschenmoser, A. Chemistry of Corphinoids. *Ann. N.Y. Acad. Sci.* **1986**, *471*, 108−129. (d) Smith, K. M.; Simpson, D. J. Raney Nickel Reductions of Chlorophyll Derivatives: Hydroporphyrins in the Anhydro Series. *J. Am. Chem. Soc.* **1987**, *109*, 6326−6333.

https://doi.org/10.1021/acs.joc.2c01202
J. Org. Chem. 2022, 87, 12096−12108

(e) Lahiri, G. K.; Stolzenberg, A. M. Reductive Chemistry of Nickel Facile Preparation of Hexahydroporphyrin Complexes by Reduction of (Octaethylisobacteriochlorin)Nickel(II). *Angew. Chem., Int. Ed. Engl.* **1993**, *32*, 429−432.
(19) De Voss, J. J.; Leeper, F. J.; Battersby, A. R. Synthetic Studies Relevant to Biosynthetic Research on Vitamin B_{12}. Part 12. Modification of the Periphery of Chlorins and Isobacteriochlorins. *J. Chem. Soc., Perkin Trans. 1* **1997**, 1105−1116.
(20) (a) Waditschatka, R.; Diener, E.; Eschenmoser, A. Chemistry of Pyrrocorphins: Carbon Methylation of Pyrrocorphinates on the Ligand Periphery. *Angew. Chem., Int. Ed.* **1983**, *22*, 631−632. (b) Schwesinger, R.; Waditschatka, R.; Rigby, J.; Nordmann, R.; Schweizer, W. B.; Zass, E.; Eschenmoser, A. Das Pyrrocorphin-Ligandsystem: Synthese des 2,2,7,7,12,12,17-Heptamethyl-2,3,7,8,12,13-Hexahydroporphyrins. *Helv. Chim. Acta* **1982**, *65*, 600−610.
(21) Kratky, C.; Waditschatka, R.; Angst, C.; Johansen, J. E.; Plaquevent, J. C.; Schreiber, J.; Eschenmoser, A. Die Sattelkonformation der Hydroporphinoiden Ni(II)-Komplexe: Struktur, Ursprung, und Stereochemische Konsequenzen. *Helv. Chim. Acta* **1985**, *68*, 1312−1337.
(22) Abraham, R. J.; Medforth, C. J.; Smith, K. M.; Goff, D. A.; Simpson, D. J. NMR Spectra of Porphyrins. Part 31. Ring Currents in Hydroporphyrins. *J. Am. Chem. Soc.* **1987**, *109*, 4786−4791.
(23) (a) Summers, J. S.; Stolzenberg, A. M. The *cis*-Influence of Hydroporphyrin Macrocycles on the Axial Ligation Equilibria of Co(II) and Zn(II) Porphyrin Complexes. *J. Am. Chem. Soc.* **1993**, *115*, 10559−10567. (b) Stolzenberg, A. M.; Stershic, M. T. Reductive Chemistry of Nickel Hydroporphyrins. Evidence for a Biologically Significant Difference Porphyrins, Hydroporphyrins, and Other Tetrapyrroles. *J. Am. Chem. Soc.* **1988**, *110*, 6391−6402. (c) Stolzenberg, A. M.; Stershic, M. T. Reductive Chemistry of Nickel Hydroporphyrins: The Nickel(I) Octaethylisobacteriochlorin Anion. *Inorg. Chem.* **1987**, *26*, 3082−3083.
(24) (a) Ide, Y.; Kuwahara, T.; Takeshita, S.; Fujishiro, R.; Suzuki, M.; Mori, S.; Shinokubo, H.; Nakamura, M.; Yoshino, K.; Ikeue, T. Nickel (II) Pyrrocorphin: Enhanced Binding Ability in a Highly Reduced Porphyrin Complex. *J. Inorg. Biochem.* **2018**, *178*, 115−124. (b) Silva, A. M. G.; Tomé, A. C.; Neves, M. G. P. M. S.; Silva, A. M. S.; Cavaleiro, J. A. S. 1,3-Dipolar Cycloaddition Reactions of Porphyrins with Azomethine Ylides. *J. Org. Chem.* **2005**, *70*, 2306−2314.
(25) Peters, M. K.; Röhricht, F.; Näther, C.; Herges, R. One-Pot Approach to Chlorins, Isobacteriochlorins, Bacteriochlorins, and Pyrrocorphins. *Org. Lett.* **2018**, *20*, 7879−7883.
(26) Yu, Y.; Furuyama, T.; Tang, J.; Wu, Z.-Y.; Chen, J.-Z.; Kobayashi, N.; Zhang, J.-L. Stable Iso-Bacteriochlorin Mimics from Porpholactone: Effect of a β-Oxazolone Moiety on the Frontier π-Molecular Orbitals. *Inorg. Chem. Front.* **2015**, *2*, 671−677.
(27) (a) Inhoffen, H. H.; Nolte, W. Chlorophyll, Hemin, XXIV Oxidative Rearrangements of Octaethylporphine to Geminiporphine Polyketones. *Justus Liebigs Ann. Chem.* **1969**, *725*, 167−176. (b) Chang, C. K. Synthesis and Characterization of Alkylated Isobacteriochlorins, Models of Siroheme and Sirohydrochlorin. *Biochemistry* **1980**, *19*, 1971−1976. (c) Chaudhri, N.; Guberman-Pfeffer, M. J.; Li, R.; Zeller, M.; Brückner, C. Pyrrocorphins of Graded Aromaticity. *Chem. Sci.* **2021**, *12*, 12292−12301.
(28) Schnable, D.; Chaudhri, N.; Li, R.; Zeller, M.; Brückner, C. Evaluation of Octaethyl-7,17-Dioxobacteriochlorin as a Ligand for Transition Metals. *Inorg. Chem.* **2020**, *59*, 2870−2880.
(29) (a) Hartwich, G.; Fiedor, L.; Simonin, I.; Cmiel, E.; Schäfer, W.; Noy, D.; Scherz, A.; Scheer, H. Metal-Substituted Bacteriochlorophylls. 1. Preparation and Influence of Metal and Coordination on Spectra. *J. Am. Chem. Soc.* **1998**, *120*, 3675−3683. (b) Chen, C.-Y.; Sun, E.; Fan, D.; Taniguchi, M.; McDowell, B. E.; Yang, E.; Diers, J. R.; Bocian, D. F.; Holten, D.; Lindsey, J. S. Synthesis and Physicochemical Properties of Metallobacteriochlorins. *Inorg. Chem.* **2012**, *51*, 9443−9464.
(30) Jentzen, W.; Song, X.-Z.; Shelnutt, J. A. Structural Characterization of Synthetic and Protein-Bound Porphyrins in Terms of the Lowest-Frequency Normal Coordinates of the Macrocycle. *J. Phys. Chem. B* **1997**, *101*, 1684−1699.
(31) Shelnutt, J. A.; Song, X.-Z.; Ma, J.-G.; Jentzen, W.; Medforth, C. J. Nonplanar Porphyrins and Their Significance in Proteins. *Chem. Soc. Rev.* **1998**, *27*, 31−42.
(32) Kingsbury, C. J.; Senge, M. O. The shape of porphyrins. *Coord. Chem. Rev.* **2021**, *431*, 213760.
(33) (a) Hood, D.; Niedzwiedzki, D. M.; Zhang, R.; Zhang, Y.; Dai, J.; Miller, E. S.; Bocian, D. F.; Williams, P. G.; Lindsey, J. S.; Holten, D. Photophysical Characterization of Tolyporphin a, Anaturally Occurring Dioxobacteriochlorin, and Synthetic Oxobacteriochlorin Analogues. *Photochem. Photobiol.* **2017**, *93*, 1204−1215. (b) Brückner, C.; Chaudhri, N.; Nevonen, D. E.; Bhattacharya, S.; Graf, A.; Kaesmann, E.; Li, R.; Guberman-Pfeffer, M. J.; Mani, T.; Nimthong-Roldán, A.; Zeller, M.; Chauvet, A. A. P.; Nemykin, V. Structural and Photophysical Characterization of All Five Constitutional Isomers of the Octaethyl-β,β'-Dioxo-Bacterio- and -Isobacteriochlorin Series. *Chem.—Eur. J.* **2021**, *27*, 16189−16203.
(34) Mass, O.; Ptaszek, M.; Taniguchi, M.; Diers, J. R.; Kee, H. L.; Bocian, D. F.; Holten, D.; Lindsey, J. S. Synthesis and Photochemical Properties of 12-Substituted versus 13-Substituted Chlorins. *J. Org. Chem.* **2009**, *74*, 5276−5289.
(35) (a) Kleinpeter, E.; Koch, A.; Schulz, S.; Wacker, P. Interplay of Para- and Diatropic Ring Currents [(Anti)aromaticity] of macrocyclic Rings Subject to Conformational Influences, Further Annelation and Hydrogenation of Aromatic Ring Moieties. *Tetrahedron* **2014**, *70*, 9230−9239. (b) Chaudhri, N. G.-P.; Zeller, M.; Brückner, C. Stepwise Reduction of β-Trioxopyrrocorphins: Collapse of the Oxo-Induced Macrocycle Aromaticity. *J. Org. Chem.* **2022**, *87*, 7179−7192.
(36) Fliegl, H.; Valiev, R. R.; Pichierri, F.; Sundholm, D. M. B. Theoretical Studies as a Tool for Understanding the Aromatic Character of Porphyrinoid Compounds. *Chem. Modell.* **2018**, *14*, 1−42.
(37) Schröder, M.; Griffith, W. P. Studies of Transition-Metal Oxo- and Nitrido-Complexes. Part 4. Reactions of Osmium Tetraoxide with Alkynes and Dienes in the Presence of Tertiary Amines. *J. Chem. Soc., Dalton Trans.* **1978**, 1599−1602.
(38) Furniss, B. S.; Hannaford, A. J.; Smith, P. W. G.; Tatchell, A. R. *Vogel's Textbook of Practical Organic Chemistry*, 5th ed.; Longman: Essex, GB, 1989; p 549.
(39) Spellane, P. J.; Gouterman, M.; Antipas, A.; Kim, S.; Liu, Y. C. Electronic Spectra and Four-Orbital Energies of Free-Base, Zinc, Copper, and Palladium Tetrakis(perfluorophenyl)porphyrins. *Inorg. Chem.* **1980**, *19*, 386−391.

https://doi.org/10.1021/acs.joc.2c01202
J. Org. Chem. 2022, 87, 12096−12108